MAJOR PROJECT-2 REPORT

ON

"EFFECT OF LOCALIZED BLADE ROUGHNESS WITH DIFFERENT VELOCITIES IN AN AXIAL FLOW COMPRESSOR CASCADE"

BY

DAMYANTI SATYAVANA

(2K11/THE/24)

Under the Supervision of

Prof. SAMSHER AND Dr. MANJUNATH

Submitted in partial fulfillment for the award of the degree of

MASTER OF TECHNOLOGY

IN

THERMAL ENGINEERING

TO THE

DEPARTMENT OF MECHANICAL ENGINEERING

DELHI TECHNOLOGY UNIVERSITY

(FORMERLY DELHI COLLEGE OF ENGINEERING)

JUNE 2014

DECLARATION

Date:

I hereby declare that the work presented in this report Titled "EFFECT OF LOCALIZED BLADE ROUGHNESS WITH DIFFERENT VELOCITIES IN AN AXIAL FLOW COMPRESSOR CASCADE" has been carried out by me under the supervision of Prof. Samsher, Professor and Dr. Manjunath, Assistant Professor Department of Mechanical Engineering, Delhi Technological University is submitted for the partial fulfillment for the award of degree of Master of Technology in Thermal Engineering (Mechanical) at Delhi Technological University, has not been submitted for the award of any other degree elsewhere.

Damyanti Satyavana
2k11/THE/24
M.Tech (Thermal Engg.)

CERTIFICATE

This is to certify that the project entitled, **"Effect of localized surface roughness of blade with different inlet velocity in an axial flow Compressor Cascade"** is submitted by **Damyanti Satyavana(Roll no. 2K11/THE/24)** to Delhi Technological University, Delhi for the evaluation of M.Tech Major Project-II as per academic curriculum. It is a record of bonafide research work carried out by student under our supervision and guidance, towards partial fulfillment of the requirement for the award of Master of Technology degree in thermal engineering.

The work is original as it has not been submitted earlier in part or full for any purpose before.

Date: 17/7/14

Dr. Samsher
Professor, Mech. Engg. Deptt.
Delhi Technological University
Delhi - 110042

Dr. K. Manjunath
Asst. Professor, Mech. Engg. Deptt.
Delhi Technological University
Delhi - 110042

ACKNOWLEDGEMENT

I would like to thank Prof. SAMSHER and Dr Manjunath sirs for giving the opportunity to work on this project. Also, They are invaluable resource for insight and guidance when looking for solutions to problems. Without their experience with blow down facilities this project would not have succeeded.

I conclude thereby, with my heartiest thanks to all my friends and well wishers who directly or indirectly assisted me in achieving completion of task.

Damyanti Satyavana
2k11/THE/24
M.Tech (Thermal Engg.)

ABSTRACT

A computational study has been conducted for different inlet velocities in linear axial flow Compressor Cascade focusing mainly on analysis of the effect of Localized blade roughness with different velocities on the aerodynamic performance of the Cascade. Measurement of pressure loss was carried out for various values of velocities with different Localized roughness on the blades of Cascade because the roughness on the blade surfaces can never be same. Except this the effect of different inlet velocities on pressure losses are also analyzed.

The Gambit 2.4.6® was used for creating geometry and computational fluid dynamics (CFD) commercial software FLUENT 6.2.16 was used to solve the governing equations. Initially, both surfaces of the blades of the cascade are kept as smooth and total pressure loss is analyzed for the different velocities like 250m/s, 300m/s and 350m/s. Then Suction surfaces and Pressure surfaces are kept as smooth separately for the inlet velocities 250m/s, 300m/s and 350m/s and Percentage profile losses are found. Then Suction and Pressure surfaces are divided into three equal parts and different roughnesses are given on the surfaces and % Profile losses are found for different inlet velocities as 250m/s, 300m/s, and 350m/s.

It is observed that for the smooth and rough blades Profile loss reduced with the increase of inlet velocity but this reduction in Profile losses is very less. But with the Localized roughness the Profile loss changes considerably.

It is observed that Profile loss in case of **Smooth blades** for the inlet velocity from 250 m/s to 300 m/s is reduced by 7.02 %.

For the wholly rough, only suction surface rough and only pressure surface rough Profile loss for the same inlet velocity increase is reduced by about 6.98 %.

In case of localized roughness profile loss reduced by about 3.6 %.

CONTENTS

LIST OF FIGURES

LIST OF TABLES

NOMENCLATURE

ρ	Density (kg/m^3)
P	Static Pressure (Pa)
E	Energy term
h	Enthalpy (kj/kg-k)
m_j	mass fraction (kg)
M	Mach number
P_{2s}	Static pressure at outlet (Pa)
P_{o1}	Total pressure at inlet (Pa)
P_{o2}	Total pressure at outlet (Pa)
γ	Ratio of specific heats for air
ζ_y	Local energy loss coefficient
S	span (mm)
Y	distance along pitch (mm)
S11, S12, S13	Partition of suction side of blade
P11, P12, P13	Partition of pressure side of blade

CHAPTER-1

INTRODUCTION

1.1 BACK GROUND

1.1.1 Cascade Nomenclature:

A flow through cascade is a flow through a row of blades. If these blades are arranged in a straight line then it is knows as "rectilinear cascade" and if blades are arranged in annular, then it is known as "annular cascade". The "annular cascade" is more towards a real-life situation. When the flow through blades is in the radial direction (inward or outward), then it is known as a "radial cascade".

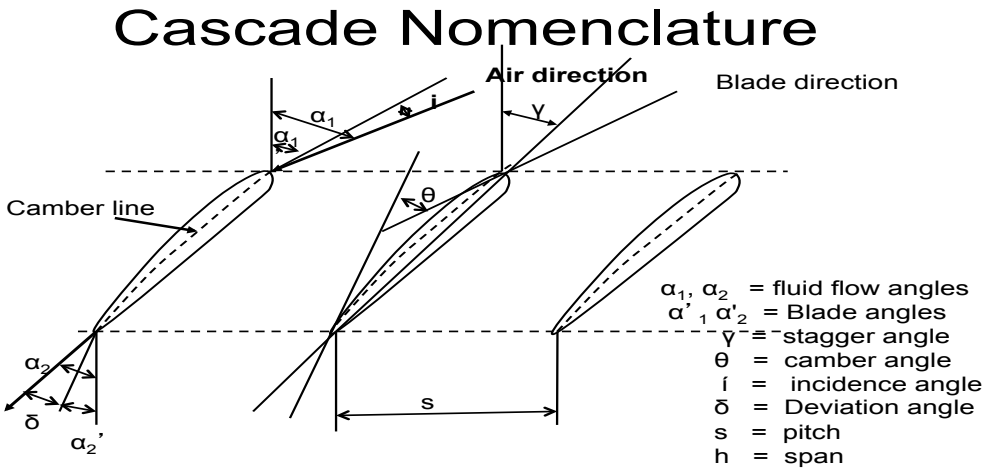

Fig. 1.1: A compressor cascade (S M YAHYA 2002)

In the fig. 1.1 the dotted line indicates the camber line. Cascade geometry is defined completely by the aerofoil specification, pitch-chord ratio and the stagger angle λ as shown in the figure 1.1.

Two-dimensional flow through a cascade is shown in the figure 1.2. Pressure side and suction side of the blades are also shown in this figure.

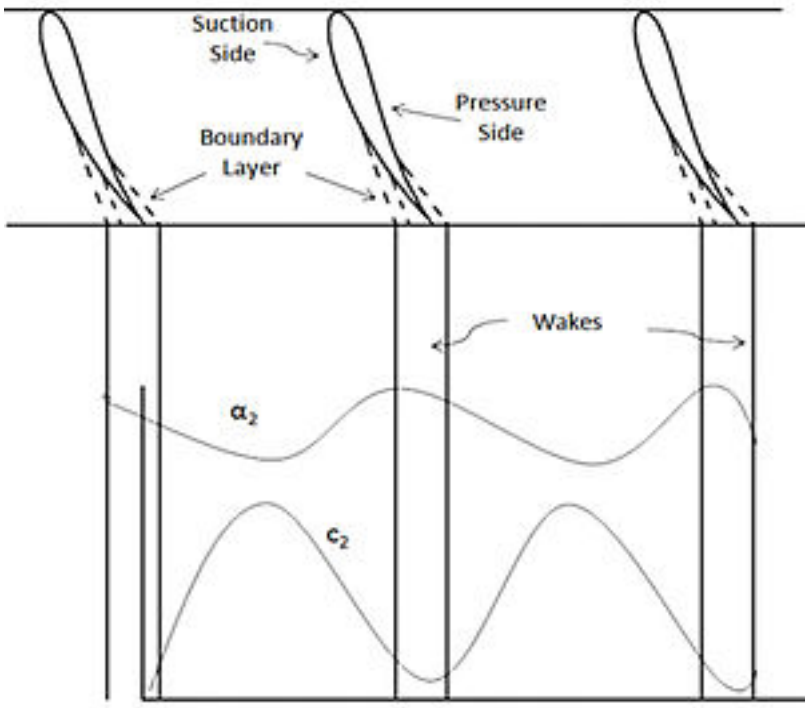

Fig 1.2:Two dimensional flow through a cascade(S M YAHYA 2002)

1.1.2 Cascade of blades:

Blades of a desired size and shape are assembled in a straight line or annular according to the cascade required. For assembling the blades, pitch(s) and stagger angle (γ) is defined. Blades of equal lengths are used in constructing a cascade. Blades for a cascade can be manufactured from wood, epoxy resin, glass wool, araldite or aluminium. Sometimes blades are made hollow to reduce the quantity of material and the weight of the blade.

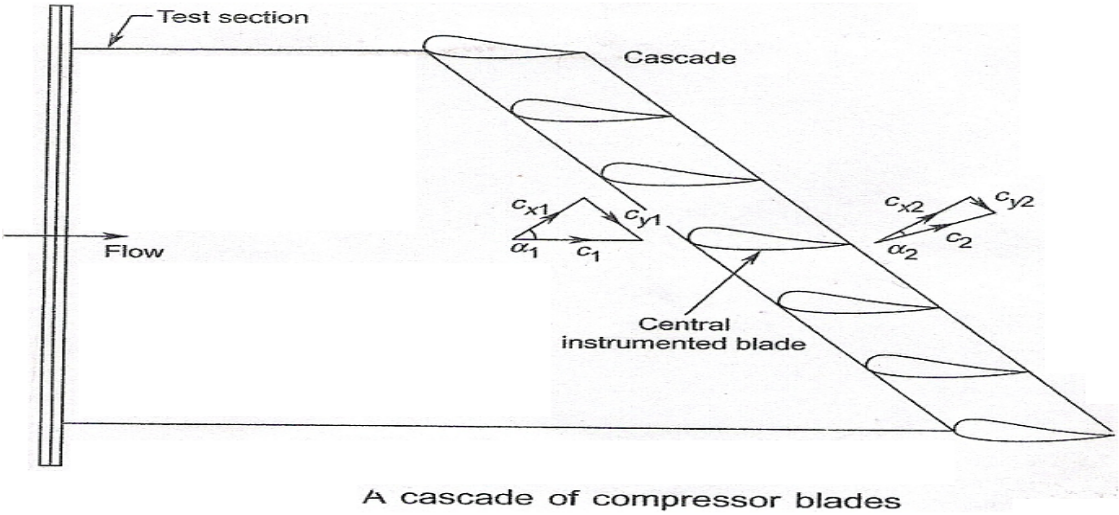

Fig 1.3: Compressor cascade(S M YAHAH 2002)

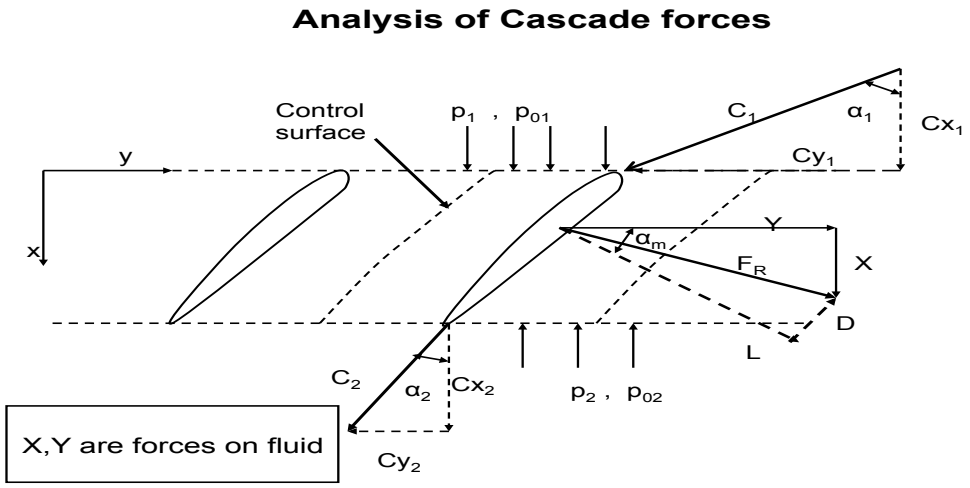

Fig: 1.4: Analyses of Cascade Forces (S M YAHAH)

In the figure 1.4 inlet and outlet velocity triangles on the blade surfaces are shown. The absolute inlet velocity is C_1 and absolute outlet velocity is C_2.

The components of C1 and C2 velocities in axial and perpendicular directions are Cy_1, Cx_1 and Cy_2, Cx_2 respectively.

1.1.3 Blade forces:

Lift force:

The perpendicular component of the mean velocity C_m is known as the lift force. The magnitude of lift force is given by the following relation---

$$L = [0.5\rho l(c_m)^2]2(s/l)\cos \alpha_m(\tan \alpha_2 + \tan \alpha_1) + s\Delta p_0 \sin \alpha_m$$

Drag force:

The parallel component of the mean velocity C_m is known as the drag force is given by-----

$$D= s\Delta p_0 \cos \alpha_m$$

Tangential Forces:

The tangential force on the blade is equal to the rate of change of momentum in the tangential direction is given by the following relation---

$$F_Y= 0.5[\rho l(c_{xm})^2]2(s/l)(\tan \alpha_1 +\tan \alpha_2)$$

Axial Forces:

The axial force takes place due to both the pressure difference and change of

momentum in the axial direction is given by the following relation----

$$Fx = [0.5\rho l(c_2)^2](s/l)\cos^2 \alpha_2 (\tan^2 \alpha_2 - \tan^2 \alpha_1) + s\Delta p_0$$

1.1.4 Blades of compressor and turbine:

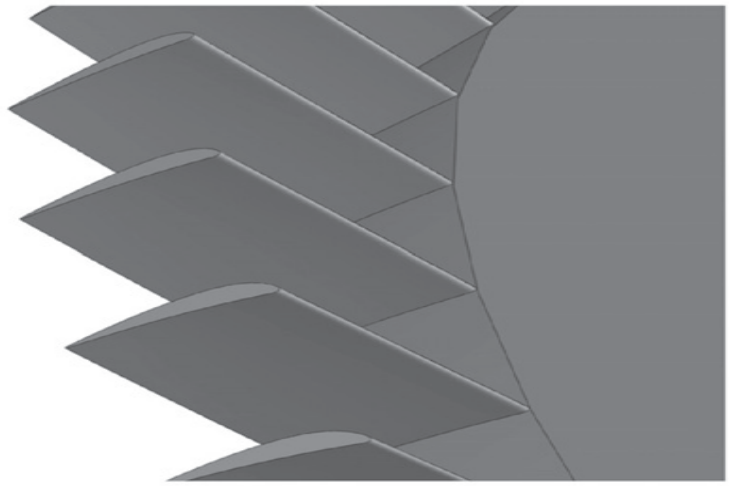

Fig 1.5: 3D compressor blade stacked along the center of gravity (CG)

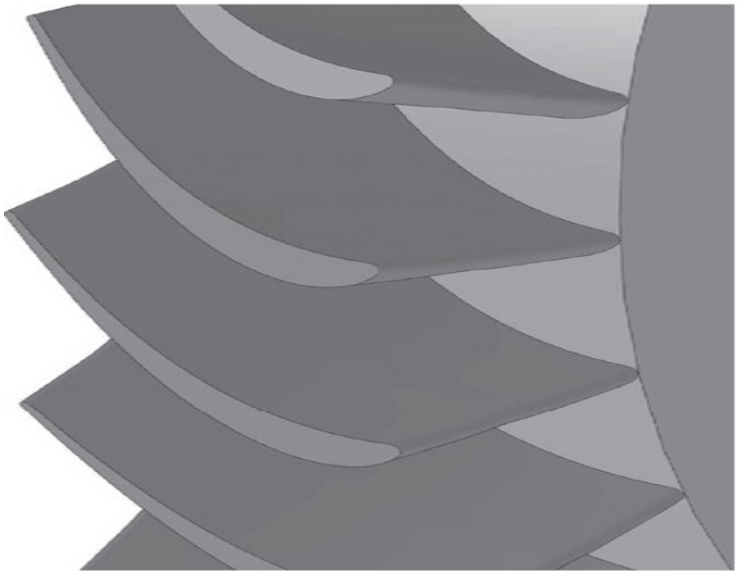

Fig 1.6: 3D turbine blade stacked along the center of gravity (CG)

1.1.5 Efficiency of a compressor cascade:

Efficiency of compressor cascade can be defined as

$$\eta = (P_2 - P_1) / (1/2)\rho(C_1^2 - C_2^2) \quad (1.1)$$

$$\Delta Po = Po_1 - Po_2 = \{P_1 + (1/2)\rho C_1^2\} - \{P_2 + (1/2)\rho C_2^2\}$$

pressure loss :

$$(P_1 - P_2) = \Delta P_0 - (1/2)\rho(C_1^2 - C_2^2)$$

$$(P_2 - P_1) = -\Delta P_0 + (1/2)\rho(C_1^2 - C_2^2)$$

$$\eta = \{-\Delta P_0 + (1/2)\rho(C_1^2 - C_2^2)\}/(1/2)\rho(C_1^2 - C_2^2)$$

$$\eta = 1 - \{\Delta P_0\} / \{(1/2)\rho(C_1^2 - C_2^2)\}$$

Since

$$C_1^2 - C_2^2 = (C^2_{X1} + C^2_{Y1}) - (C^2_{X2} + C^2_{Y2})$$

$$= C^2_{y1} - C^2_{y2} \quad = (C_{y1} + C_{y2})(C_{y1} - C_{y2}) \quad C_{Ym} = (C_{Y1} + C_{Y2})/2$$

$$C^2_1 - C^2_2 = 2\, C_{Ym}.\, (C_{y1} - C_{y2}) = 2C^2_x \tan(\alpha_m)(\tan\alpha_1 - \tan\alpha_2)$$

Efficiency

$$\eta = 1 - [\Delta Po / \{\rho C^2_X \tan(\alpha_m)(\tan\alpha_1 - \tan\alpha_2)\}] \quad (1.2)$$

Substituting the value of $\Delta P_0 = (1/2)\rho C^2_X.\, \zeta$

And the value of $C_f = 2(\tan\alpha_1 - \tan\alpha_2)$

$$\eta = 1 - \{(1/2)\rho C_x^2.\zeta / \rho C_x^2 \tan(\alpha_m).Cf/2\}$$

$$\eta = 1 - [\zeta / Cf \tan\alpha_m]$$

$$C_L / C_D = (C_f/\zeta)\sec^2\alpha_m$$

$$\eta = 1 - [C_D \sec^2\alpha_m / C_L \tan\alpha_m$$

$$\eta = 1 - [2C_D/C_L \sin 2\alpha_m] \quad (1.3)$$

1.1.6 Maximum efficiency of a cascade:

Let C_D/C_L=Constant

$$\left(\frac{d\eta}{d\alpha m}\right)_{max} = \cos 2\alpha_m = 0$$

$$\cos 2\alpha_m = \cos 90^o$$

$$2\alpha_m = 90^o$$

$$\alpha_m = 45^o$$

Hence $(\eta_D)max = 1 - [2C_D / C_L]$ (1.4)

Where, C_D=Co-efficient of Drag and

C_L= Co-efficient of Lift.

Flows in actual turbo machine is three dimensional due to rotation and boundary layer formation. To make the problem easy we assuming the flow to be two dimensional by neglecting the blade height. In axial machines flow is assumed to be two dimensional flow.In three dimensional flow is reduced to two dimensional plane flow in which variations occur only in pitchwise and streamwise directions only.

The velocity (C_2) and angle (α_2) profiles at the exit of a cascade with two-dimensional flow are remains constant at all blade heights.

1.2 Motivation

The material in this report originated from attempts to study, to understand and to analyze the effect of blade roughness on the performance of an axial flow compressor cascade in real life situation. Because the performance of a compressor differs when it goes through in operations for a long time. The blades of a compressor cascade becomes rough with the passing time due to many reasons such as due to erosion effect of many types of particles, and due to deposition of particles etc.

1.3 Problem statement:

The primary object of this project is to use the computational software with the aim of study of the localized roughness with the various inlet velocities on the percentage pressure loss on the compressor cascade. Two-dimensional Model of compressor cascade geometry was made with the help of Gambit® 2.2.3 as pre processor & FLUENT® 6.2 is be used as solver & post processor for flow simulation. On the model of rectilinear cascade of compressor blades, discretization has been done with the help of Gambit®. Then Fluent® was used on the flow through the blades. From the simulation results relation between velocity and percentage pressure loss had been studied for the smooth blade and rough blade. This work was done in order to find out the effect of localized roughness with the inlet velocities on various blade surface of the compressor cascade.

CHAPTER-2
LITERATURE REVIEW

(1) Effect of boundary layer suction:

Shao-Wen Chen and Shi-jun-sun [2] studied an effect of boundary layer suction on the flow characteristic in a highly loaded Compressor cascade with a stator clearance experimentally. They applied hole type suctions with different locations and distributions on the end wall to control Clearance flow and losses.

The result shows that the clearance flow is improved and the losses reduced when boundary layer suction is adopted and the maximum loss reduction with clearance is 32%.

They observed that with a short clearance the same flow separation obtains in the corner of the suction surface as that with no clearance.

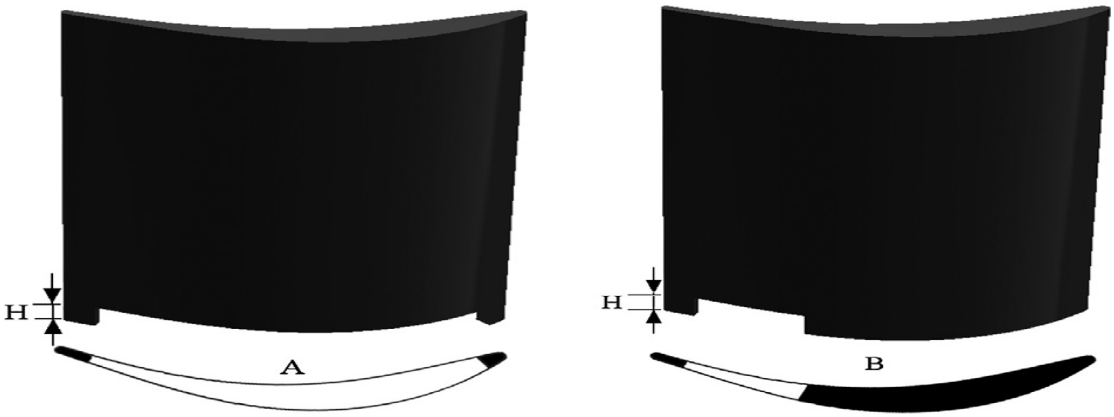

Fig 2.1: Schematic diagram of two clearance types (A: a long clearance B: a short clearance).

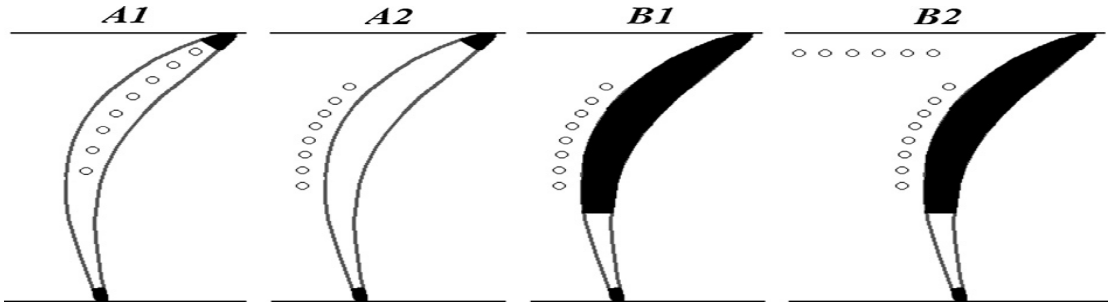

Fig 2.2: Distribution of suction holes.

It is observed that appropriate boundary layer suction can change flow pattern on the suction side and the end wall and improve the flow to reduce the losses. The loss in case A with a long clearance is 22.5% and in case B with a short clearance is 32%. Because of the suction, the flow condition becomes simpler and the corner separation is significantly suppressed and the decreases the losses significantly.

In another research **Guo Shuang and Chen Shaowen [4]** studied the effect of boundary layer suction position on the compressor cascade performance. Results shows that with higher suction flow rate and the suction position closer to the trailing edge reduces the losses and the maximum reduction in the total pressure loss is 16.5%. The effect of suction position is more than the suction flow rate in affecting the total pressure loss.

(2) Effect of depositions models:

JIA Hurxia, XI Guang, Wen Shurping [12] worked on effects of Deposition Models on Deposition and Performance Deterioration in Axial Compressor Cascade. He used partial deposition model and according to him total pressure loss co-efficient increases with the operating time/h. The effect of particle deposition on compressor performance is mainly represented by the change of the blade geometry that can be measured by the deposition thickness and the change of flow field that can be observed by the change of total pressure loss co-efficient and pressure coefficient.

He found that total pressure loss co-efficient for three angle of attack -4.3^0, 0^0, and 6.7^0. Total pressure loss co-efficient increases with increase in positive angle of attack and is maximum for 6.7^0 angle of attack.

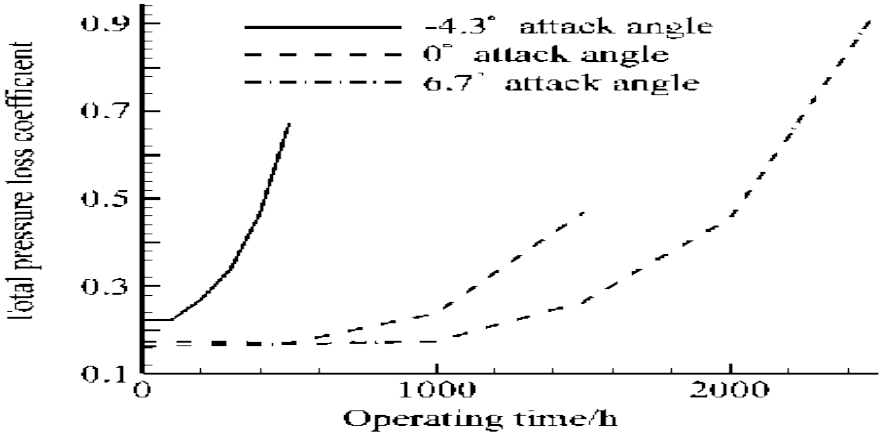

Fig 2.3: Relation between pressure loss coefficient and operating time

The result shows that the gas attack angle has effect on the particle deposition. The total pressure loss coefficient changes slowly at the beginning of operating time and then changes rapidly after some period of time.

The change of total pressure loss coefficient with operating time and the distribution of pressure co-efficient on blade surface after 500 hours was predicted by using partial deposition model.

(3) Development of flow field around the cascade:

Ahmed and Yilbas [3] was studied the development of the flow field around the cascade. They studied the boundary layer development at the suction and pressure surfaces at the different angle of attack and for different solidity. He also found the effect of leading edge rotation on stall inception of isolated airfoil.

They found that increase in solidity increases the angle of attack at which separation occurs. Lift, drag and pressure loss coefficients are affected by the angle of attack and the solidity. Rotation of the leading edge reduces the drag coefficient while it increases the lift co-efficient. The angle of attack was varied from 0 to 24 degrees and

solidity (c/s) was varied from 0.55 to 0.83. According to him high degree of flow spilling occurs at the leading edge of the airfoil for high angle of attack and results in separation at the trailing edge. The point of separation moves towards the leading edge when solidity (c/s) increases. The boundary layer thickness increases towards the trailing edge as the angle of attack increases. The rate of this increase reduces at low solidity. In the case of leading edge rotation, separation delays at high angle of attacks and diminishes as the total surface rotates. Pressure coefficient on the suction surface at the trailing edge attains higher values with incidence and with a decrease in the solidity.

(4) Effect of blade erosion:

Hamed and Tabakoff [7] studied the effect of blade roughness and tip clearance on the compressor adiabatic efficiency and the effect on the pressure ratio. The increase in the rotor tip clearance due to blade erosion was taken to be equal to 1% of the blade height and the roughness was taken for the two cases as for case-1 was 4μm and for case-2 for rotor-8μm and for stator-6μm. They predicted the loss in adiabatic efficiency was 3-4% under the combined effects of increased blade surface roughness and tip clearance due to erosion.

(5) Effect of surface roughness on end losses:

Singoria, and Samsher [5] studied the effect of surface roughness on the secondary losses in an axial flow compressor cascade. They found that with the increase of surface roughness the percentage pressure loss decreases. The percentage of secondary losses was 5.26, 5.13 and 5.06 for the roughness of 250μm is applied on suction and pressure surfaces individually and both the surfaces together while the percentage of secondary losses for the smooth blade cascade was 5.33 %, 5.17% and 5.15%.

Seung chul back and June Hyuk Sohn [8] also studied the effect of surface roughness on an axial flow compressor cascade. The measured value was taken at 0.3 chord downstream of the blade trailing edge.

For the roughness of 180µm, 300µm, 425µm, and 850µm, the axial velocity ratio across the blade row was decreased by 0.1%, 2.1%, 2.5%, and 5.4%, respectively and the exit flow angle deviation increased by 24%, 38%, 51%, and 70%, respectively.

The mass-averaged total pressure loss was increased by 12%, 44%, 132%, and 217%, respectively.

Pandey and Chakraborty [6] analyzed the flow behavior through a compressor cascade. They studied the effect of angle of attack or flow incidence angle on various flow parameters viz. static pressure, dynamic pressure, turbulence and their distribution in the flow field. They observed that the static pressure for a compressor cascade increases along the cascade flow field, while the dynamic pressure and velocity decreases.

2.2 Summary of Literature review:

Table 2.1:Summary of literature review

S.N	Author	Year	Major parameters	Exp/ Comp.	Major finding
1	Vinod Kumar Singoria, and Samsher[5]	2013	Surface roughness	Comp.	For the smooth blade Secondary losses were 5.33%, 5.17% and 5.15%.
2	Show-wen chen,Shi-jun-sun[2]	2013	High load, large incidence angle, % tip clearance, suction slot length	Exp.	Boundary layer suction,3D flow separation, secondary loss. Maximum loss reduction with clearance was 32%.
3	Jia Hurxia, XI Guang, Wen Shurping [12]	2005	Operating time, critical velocity, critical angle	Num.	Pressure loss co-efficient, pressure co-efficient distribution. Pressure loss co-efficient was maximum for 6.7^0 angle of attack.
4	N. Ahmed, B.S. Yilbas [3]	1998	Angle of attack, solidity, rotation of leading edge	Comp.	Loss in adiabatic efficiency, lift, drag and pressure loss co-efficient. Pressure coefficient on the suction surface at the trailing edge attains higher values.
5	A. Hamed and W. Tabakoff [7]	1997	Surface roughness and tip clearance	Comp.	Adiabatic efficiency, pressure loss. Loss in adiabatic efficiency was 3-4%

2.3 Gaps in Literature Review:

A lot of work has been done on the profile loss co-efficient for the compressor as well as for the turbine. Some of researchers investigated the effect of incidence angle and effect of clearance on the Pressure loss co-efficient. Some of researches investigated the effect of surface roughness of blades on the pressure loss co-efficient. But all the researches considered the surface roughness either on the wholly surface of blades or on the suction and pressure surfaces of the blades. While in the real life situation the Roughness on the blades can never be uniform. Effect of non-uniform roughness of the blades on the pressure loss co-efficient has not been studied.

CHAPTER-3
METHODOLOGY

3.1 Basic Governing Equations:

• Conservation of momentum (Navier-Stokes equation)

• Conservation of mass (Continuity equation)

• Conservation of energy (Energy Equation)

Conservation of momentum was independently constructed by Navier (1827) and Stokes (1845) and are referred to as the Navier-Stokes equation. Solution of governing equations is achieved by discretising the domain into finite control volume mesh. The governing equations are integrated over each control volume in such a way that mass, momentum, energy etc. are conserved in a discrete sense for each control volume.

3.2 Introduction to CFD

CFD is an acronym that refers to Computational Fluid Dynamics. CFD uses numerical methods to solve the fundamental nonlinear differential equations that describe fluid flow (the Navier-Stokes and allied equations), for predefined geometries and boundary conditions. The result is a wealth of predictions for flow velocity, temperature, density, and chemical concentrations for any region where flow occurs.

3.2.1 Input for CFD:

Theoretically, to analyze the fluid flow, the basic conservation equations have to be solved. The equations that govern the flow include those for the

1. Conservation of momentum (Navier-Stokes equation)
2. Conservation of mass (Continuity equation)
3. Conservation of energy (Energy Equation)

3.2.2 Discretization of Equations:

Whenever the linearization procedure is necessary, an iterative calculation procedure must be adopted, whereby the equations are successively re-linearized and solved until the solution to the original numerical form of the equations is attained.

The principal approach of CFD is to represent those equations as well as flow domain in discretized form by using one of "finite differencing", "finite element", or "finite volume methods". Each discretization scheme differs in the assumption of profile within a small volume considered and the way space is discretized. Once discretized, it leaves meshes that cover the domain and a set of algebraic equations for that control volume.

3.2.3 Outline of Any CFD Process:

There is essentially 3stage simulation process applied to any CFD code. The three stages are preprocessing, simulation and post-processing.

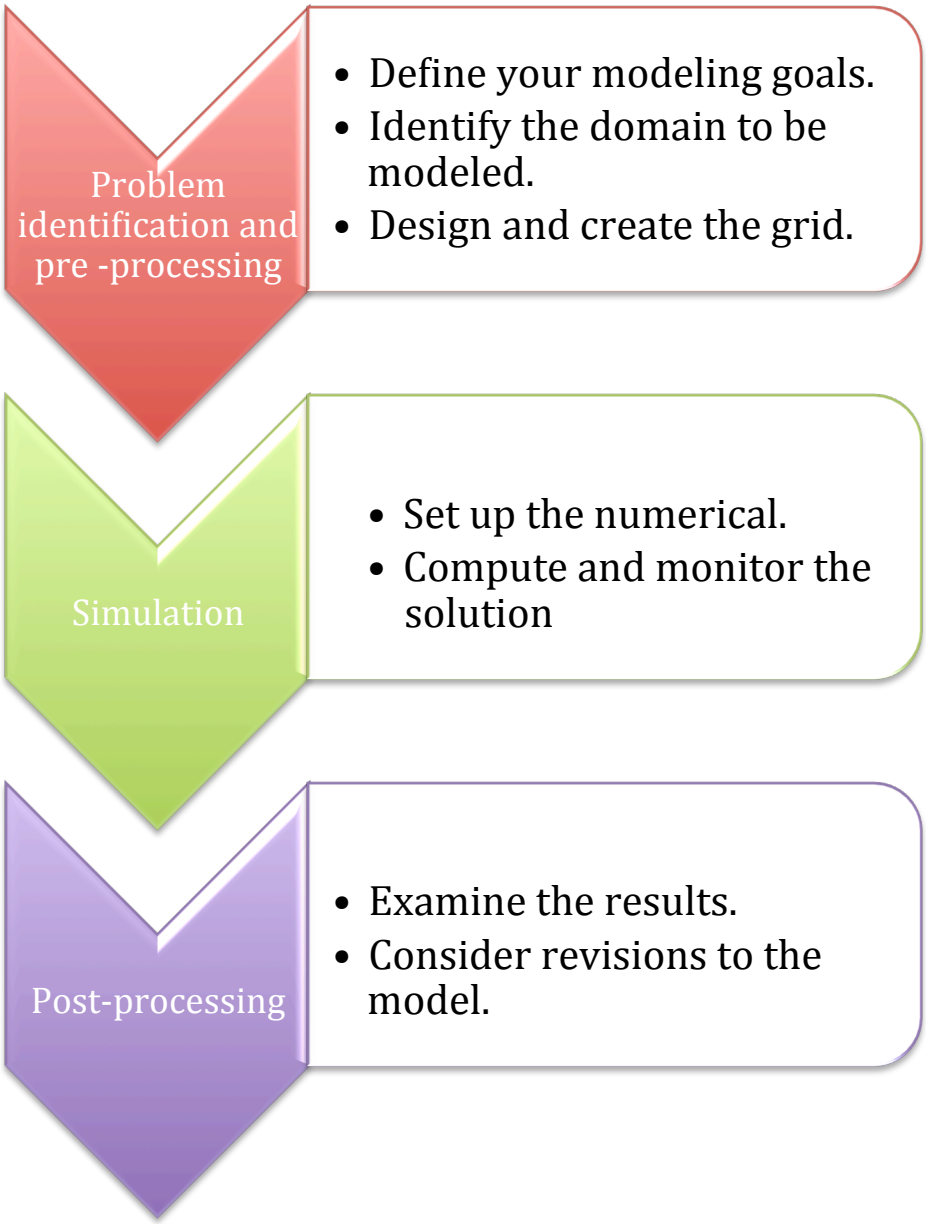

3.2.4 CFD Modeling:

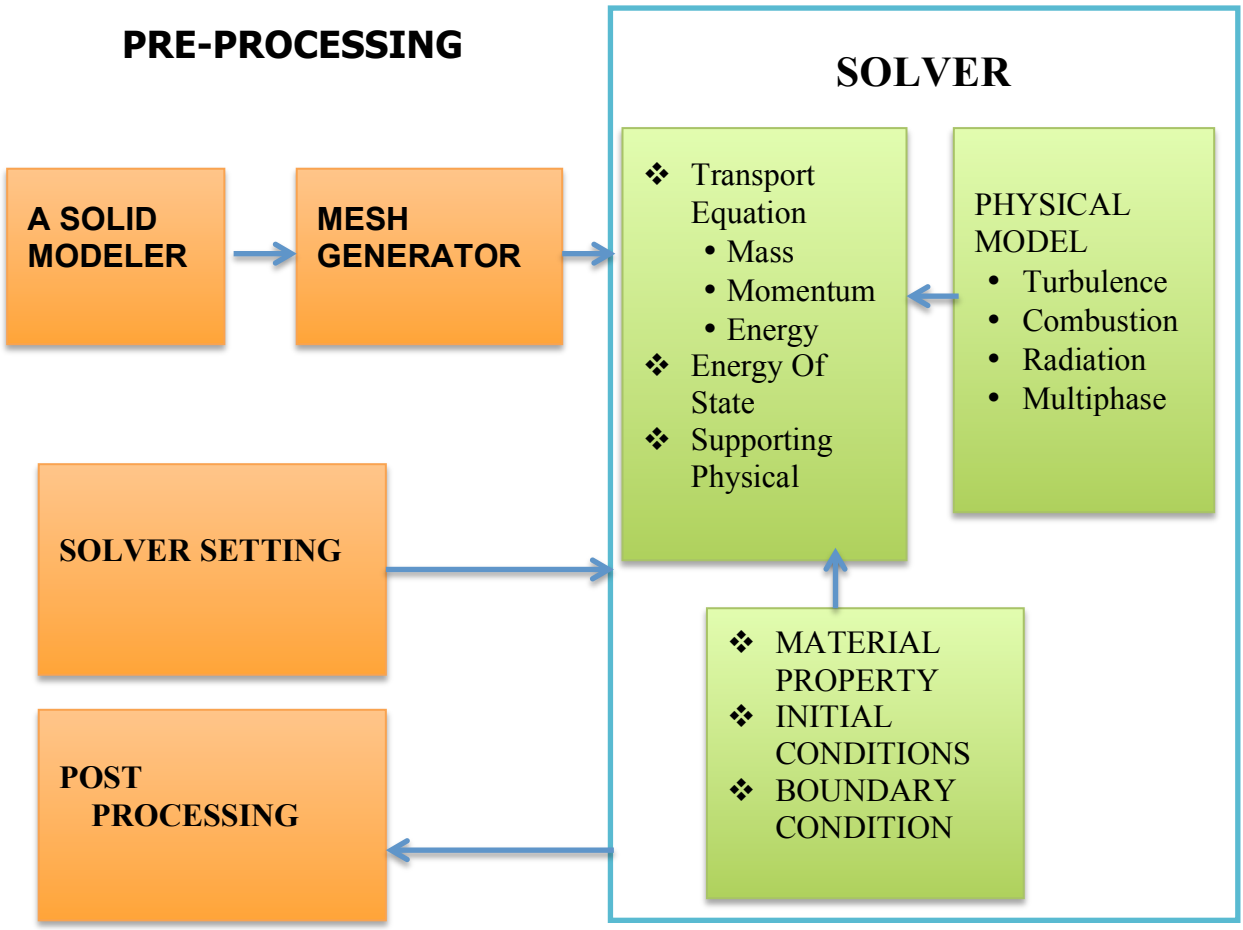

3.3 CFD analysis procedure:

Formulate the Flow Problem:

The first step of the analysis process is to formulate the flow problem by seeking answers to the following questions:

- What is the objective of the analysis?
- What is the easiest way to obtain those objective?
- What geometry should be included?
- What are the free stream and/or operating conditions?
- What dimensionality of the spatial model is required? (1D, 2D, axisymmetric, 3D)
- What should the flow domain look like?
- What temporal modeling is appropriate? (steady or unsteady)
- What is the nature of the viscous flow? (Inviscid, laminar, turbulent)

3.3.1 Model the Geometry and Flow Domain: do formatting:

The body about which flow is to be analyzed requires modeling. This generally involves modeling the geometry with a CAD software package. Approximations of the geometry and simplifications may be required to allow an analysis with reasonable effort. Concurrently, decisions are made as to the extent of the finite flow domain in which the flow is to be simulated. Portions of the boundary of the flow domain coincide with the surfaces of the body geometry.

3.3.2 Establish the Boundary and Initial Conditions:

Since a finite flow domain is specified, physical conditions are required on the boundaries of the flow domain. The simulation generally starts from an initial solution and uses an iterative method to reach a final flow field solution.

3.3.3 Establish the Simulation Strategy:

The strategy for performing the simulation involves determining such things as the use of space marching or time marching, the choice of turbulence or chemistry model, and the choice of algorithms.

The simulation requires several input files: Grid file, Initial solution file, Input data file, Auxiliary files (i.e. multi-processor, local boundary conditions, chemistry…)

3.3.4 Establish the Input Parameters and Files:

A CFD codes generally requires that an input data file be created listing the values of the input parameters consisted with the desired strategy. Further a grid file containing the grid and boundary condition information is generally required. The files for the grid and initial flow solution need to be generated.

3.3.5 Perform And Monitor the Simulation for Completion:

The simulation is performed with various possible with options for interactive or batch processing and distributed processing. As the simulation proceeds, the solution is monitored to determine if a "converged" solution has been obtained, which is iterative convergence.

3.3.6 Post-Process the Simulation to get the Results:

Post-Processing involves extracting the desired flow properties (thrust, lift, drag, etc.) from the computed flow field.

3.3.7 Make Comparisons of the Results:

The computed flow properties are then compared to results from analytic, computational, or experimental studies to establish the validity of the computed results.

3.3.8 Repeat the Process to Examine Sensitivities:

The sensitivity of the computed results should be examined to understand the possible differences in the accuracy of results and performance of the computation with respect to

- Dimensionality
- Flow conditions
- Initial conditions

3.4 Design of Cascade:

3.4.1 Geometry Creation using Gambit®:

The 2D modeling scheme was adopted in GAMBIT and it was analyzed using FLUENT. A compressor cascade model with zero degree flow angle of incidence was designed. A two dimensional model of the profile was created, with the help of Gambit®. Dimensions of the cascade & flow parameters are shown in Table. The compressor cascade used for research contains five blades and formed four complete passages, however only one passage is used for the recording and documentation of data. Chord of all the blades are 37mm and the pitch is 31.07mm.

The following table summarizes the geometric properties of the compressor cascade.

Table 3.1: Cascade Parameter

1	Aspect ratio (c/h)	0.987
2	Chord length(c)	37 units
3	Pitch of the cascade(s)	31.07 units
4	Solidity (c/s)	1.19
5	Inlet velocity	250m/s, 300m/s, 350m/s
6	Viscous models	K-epsilon
7	Software used	Gambit and Fluent
8	Type of analysis	Computational 2D
9	No of blades	5
10	No of flow channels	4
11	Working fluid	Air

All various co-ordinates of blade profile are plotted using vertex command in Gambit®. By using the edge command all the co-ordinates are joined to obtain a wire frame model. This gives us a blade of the compressor. Now rotate this blade at the stagger angle as shown in the figure 3.2.

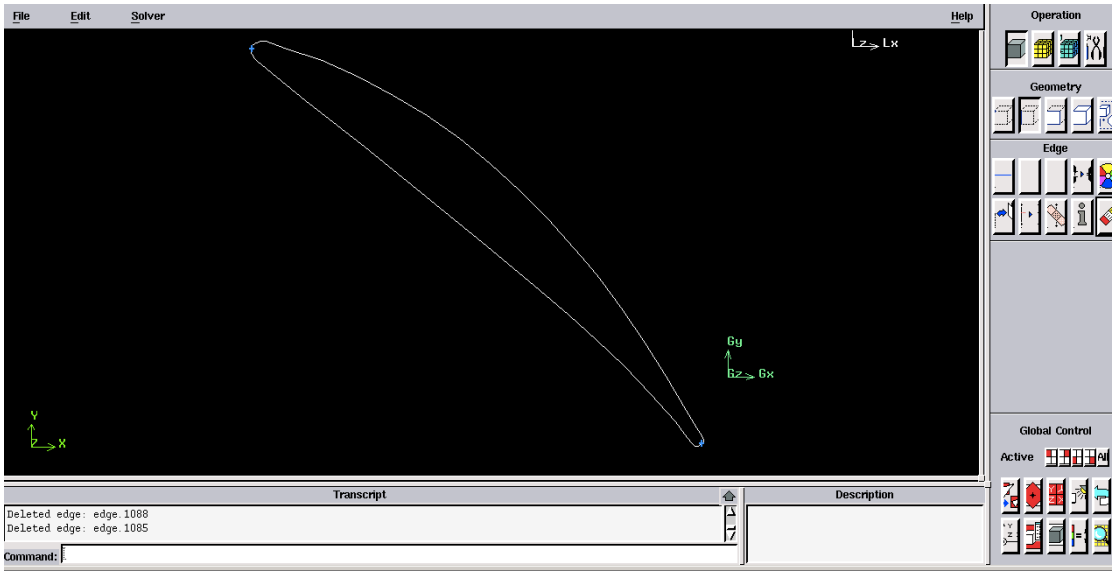

Fig 3.2: Blade of cascade

Copy this profile 4 times to get the desired cascade and now adjust the cascade to the required inlet flow angles for the shock less entry.

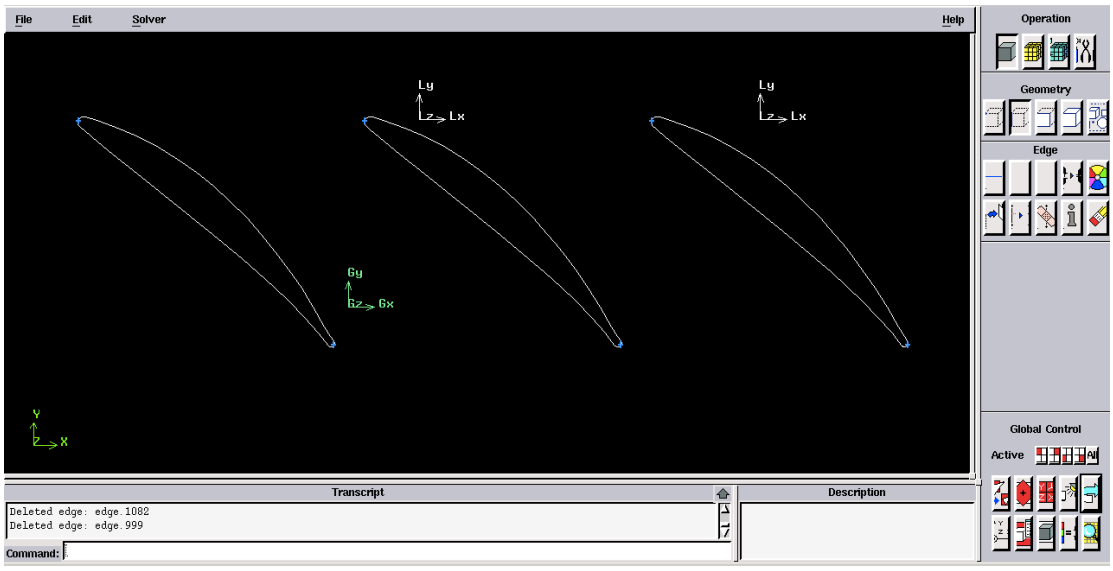

Fig 3.3: Blades of desired cascade

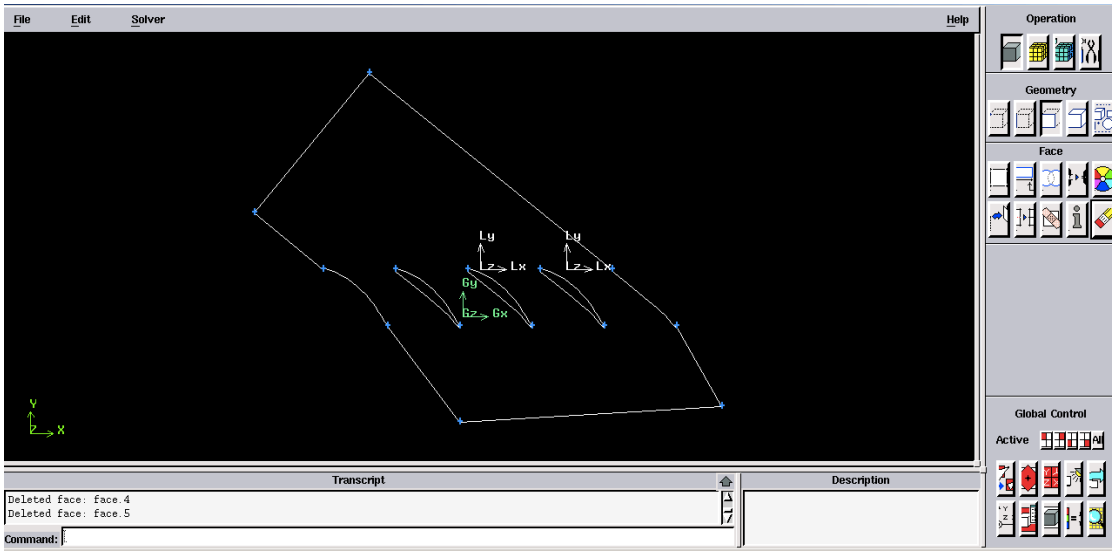

Fig 3.4: Wire frame of the cascade

Now using face command created the face and finally the face was meshed by face mesh command, by giving spacing 1.

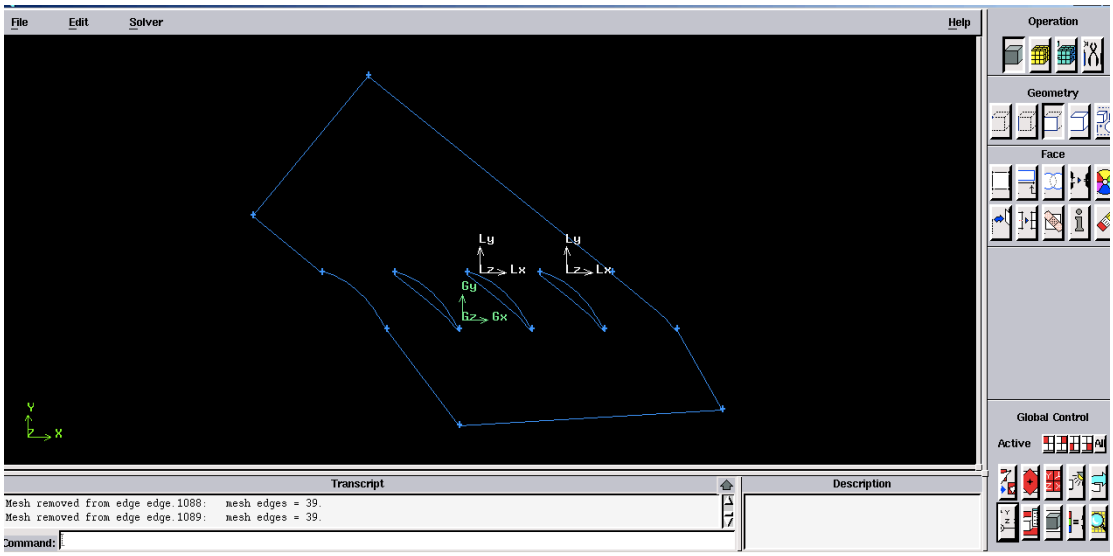

Fig 3.5: Face of the cascade

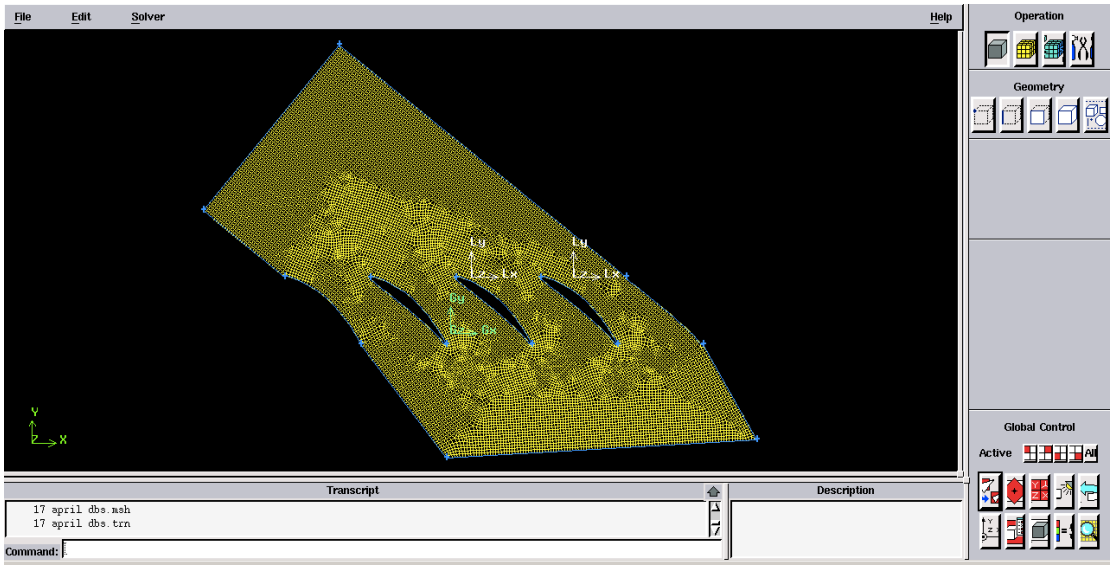

Fig 3.6: Meshing of the fluid field

Now for the computational study of the localized surface roughness suction surfaces and the pressure surfaces are divided into three parts as S-11, S-12, S-13 AND P-11, P-12, P-13 for the one blade and same for the other blades as shown in fig. 3.7 and fig. 3.8.

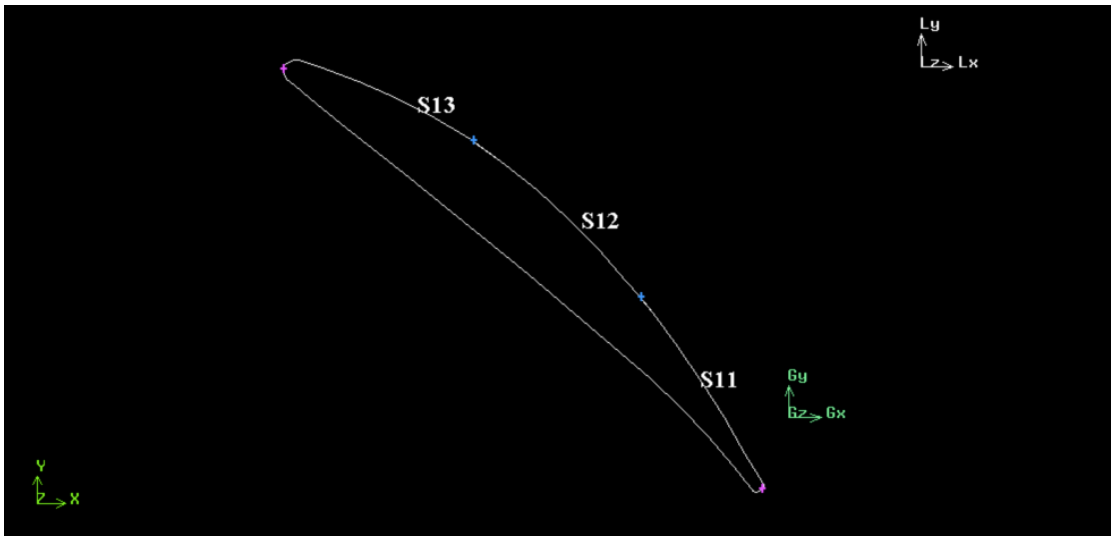

Fig. 3.7: Division of Suction surface of a blade

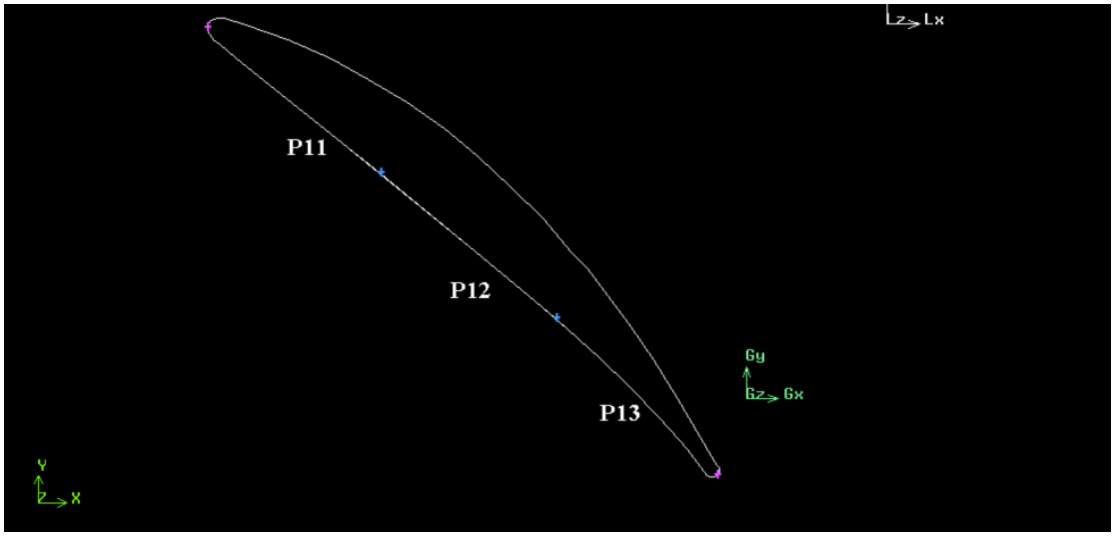

Fig. 3.8: Division of Pressure surface of a blade

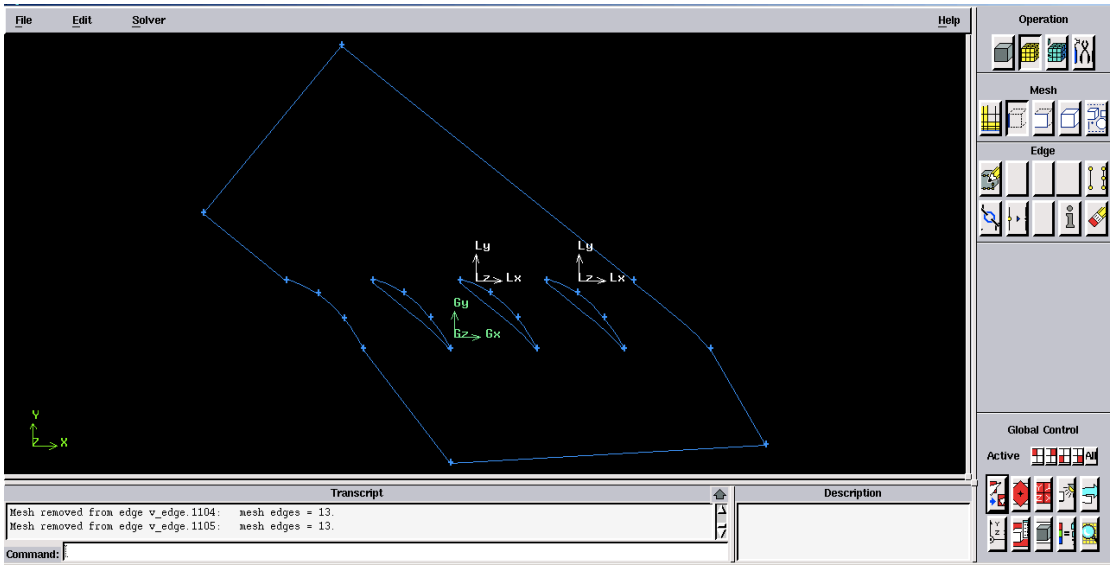

Fig 3.9: Division of Suction surfaces of blades in a Cascade.

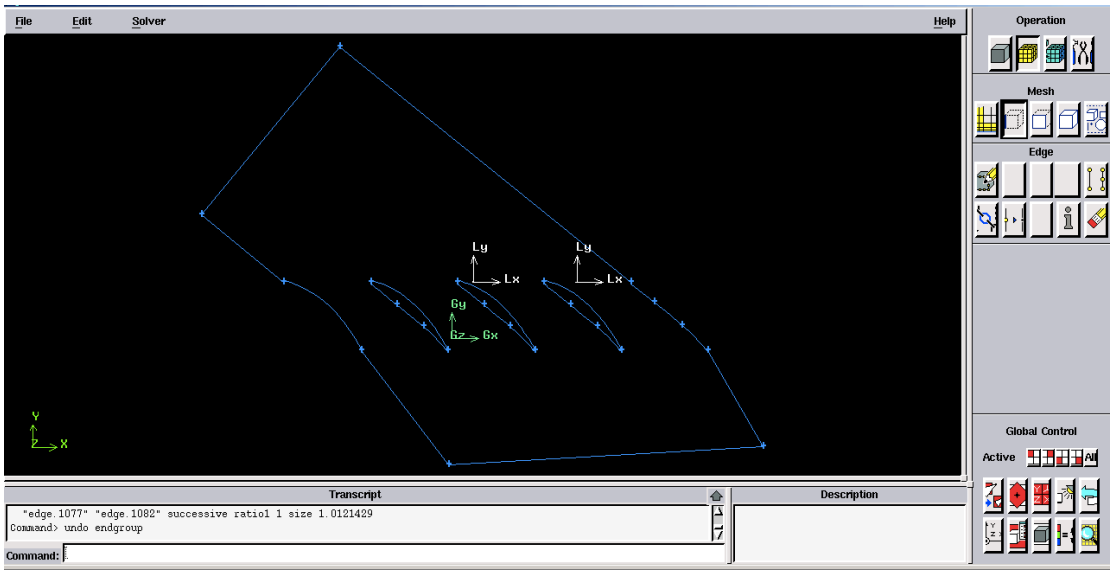

Fig 3.10: Division of Pressure surfaces of blades in a Cascade

Now the boundary types are defined. Inlet takes as velocity inlet and outlet takes as pressure outlet. All the blades are defined as wall. Then cascade is saved and then exported to mesh which will be used in fluent as case file. Grid checking and scaling of the model is done in fluent. K-epsilon realizable viscous solver model is selected. The various operating and boundary conditions are stated and the model is iterated to convergence.

3.5 Defined values:

3.5.1 Model – Viscous K-epsilon realizable model

3.5.2 Material – Air

- Density =1.225 kg/m^3
- Viscosity =1.7894e-05 kg/m-s

3.5.3. Operating conditions-

- Operating pressure = 101325 bar
- Reference pressure location X (m) = 0Reference pressure location Y (m) = 0

3.5.4 Turbulence:

- Specification method- K and Epsilon
- Turbulent kinetic energy (m^2/s^2)- 0.8
- Turbulent dissipation rate (m^2/s^2)- 0.8
- Backflow turbulent kinetic energy (m^2/s^2)- 0.8
- Backflow turbulent dissipation rate (m^2/s^2)- 0.8
-

3.5.5 Boundary conditions:

Table 3.2: Boundary conditions

S.N	BOUNDARY ZONE	BOUNDARY TYPE	DATA
1	Inlet	Velocity inlet	250m/s, 300m/s, 350m/s
2	Outlet	Pressure outlet	101325 bar
3	Suction blade 1-1	Wall	300µm
4	Suction blade 1-2	Wall	500µm
5	Suction blade 1-3	Wall	750µm
6	Suction blade 2-1	Wall	300µm
7	Suction blade 2-2	Wall	500µm
8	Suction blade 2-3	Wall	750µm
9	Suction blade 3-1	Wall	300µm
10	Suction blade 3-2	Wall	500µm

11	Suction blade 3-3	Wall	750µm
12	Suction blade 4-1	Wall	300µm
13	Suction blade 4-2	Wall	500µm
14	Suction blade 4-3	Wall	750µm
15	Pressure blade 2-1	Wall	300µm
16	Pressure blade 2-2	Wall	500µm
17	Pressure blade 2-3	Wall	750µm
18	Pressure blade 3-1	Wall	300µm
19	Pressure blade 3-2	Wall	500µm
20	Pressure blade 3-3	Wall	750µm
21	Pressure blade 4-1	Wall	300µm
22	Pressure blade 4-2	Wall	500µm
23	Pressure blade 4-3	Wall	750µm
24	Pressure blade 5-1	Wall	300µm
25	Pressure blade 5-2	Wall	500µm
26	Pressure blade 5-3	Wall	750µm

3.5.6 Measuring plane:

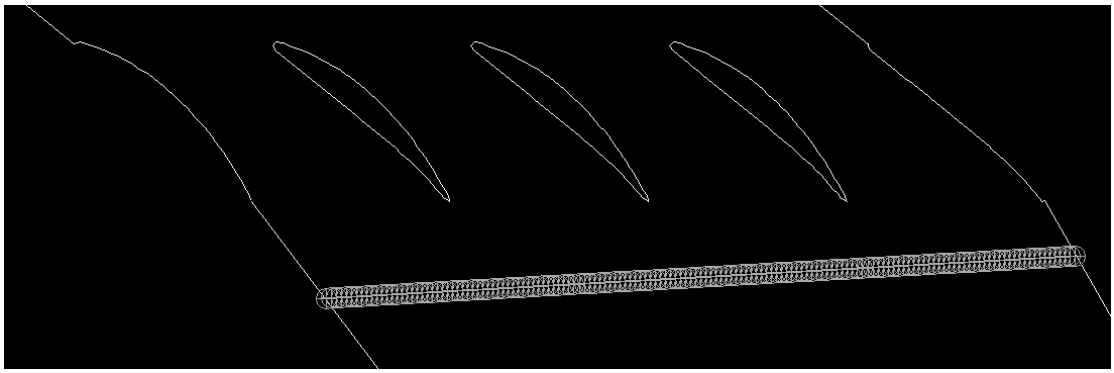

Fig 3.11: Measuring plane at 0.4 chord.

The center passage is measured in the cascade so that the potential flow effects from the top and bottom wall would be minimal. The loss coefficient is calculated and area-averaged over one passage. The values of p01, p02, p2s are found on the measuring plane from the X-Y plot and pressure loss co-efficient is find out. Then graph is plotted between pressure loss co-efficient and Y/S(non dimensional span).

The pressure loss coefficient ξ is calculated using the relation proposed by Dejc and Trojanovskij, expressed as-------

$$\xi = \left[\frac{P2S}{P01}\right]^{\frac{\gamma-1}{\gamma}} \frac{1-\left[1-\left[\frac{P01-P02}{P01-P2S}\right]\left[1-\frac{P2S}{P01}\right]\right]^{\frac{\gamma-1}{\gamma}}}{\left[1-\left[\frac{\square 2S}{P01}\right]^{\frac{\gamma-1}{\gamma}}\right]\left[1-\left[\frac{P01-P02}{P01-P2S}\right]\left[1-\frac{P2S}{P01}\right]\right]^{\frac{\gamma-1}{\gamma}}} \qquad (3.1)$$

Where, P2s = Static pressure at the outlet of cascade,

P01 = Total pressures at the inlet of cascade,

P02 = Total pressure at the outlet of cascade,

Y = Ratio of specific heats for air.

Now after finding the non-dimensional span graphs are plotted between various velocities and their corresponding profile loss co-efficient and results are analyzed.

CHAPTER-4

RESULTS AND DISCUSSION

For the computation of profile loss for different cases the compressor cascade was designed by Gambit and exported mesh of the cascade was analyzed using the Fluent 6.2 as solver and boundary types were defined in the pre-processor. The flow, pressure distribution and profile loss were analyzed at proper location. At inlet the measurement plane was taken at (-63.42, 22.80) and (60.88, 22.80) by drawing the rake line/rake option in Fluent. At the exit the measurement plane was taken at (-21.83, -19.33) and (96.33, -12.71) along the whole span, which is about 0.4 chord downstream. Required readings were taken at the measuring planes and profile losses were calculated for the different cases. On the basis of readings obtained by the simulation of flow profile loss was calculated in the excel sheet by using Dejc and Trojanovskij (1973) relation (4.1).

$$\xi = \left[\frac{P2S}{P01}\right]^{\frac{\gamma-1}{\gamma}} \frac{1-\left[1-\left[\frac{P01-P02}{P01-P2S}\right]\left[1-\frac{P2S}{P01}\right]\right]^{\frac{\gamma-1}{\gamma}}}{\left[1-\left[\frac{P2S}{P01}\right]^{\frac{\gamma-1}{\gamma}}\right]\left[1-\left[\frac{P01-P02}{P01-P2S}\right]\left[1-\frac{P2S}{P01}\right]\right]^{\frac{\gamma-1}{\gamma}}} \qquad (4.1)$$

Loss coefficient was calculated at mid span, where the flow is free from the effect of end wall.

4.1 Validation of simulated Results:

Average percentage profile losses were computed from simulation results along the non-dimensional pitch. Obtained Results are compared with the experimental values of % profile loss measured along the pitch by Samsher [2007] as shown in Fig 4.1.

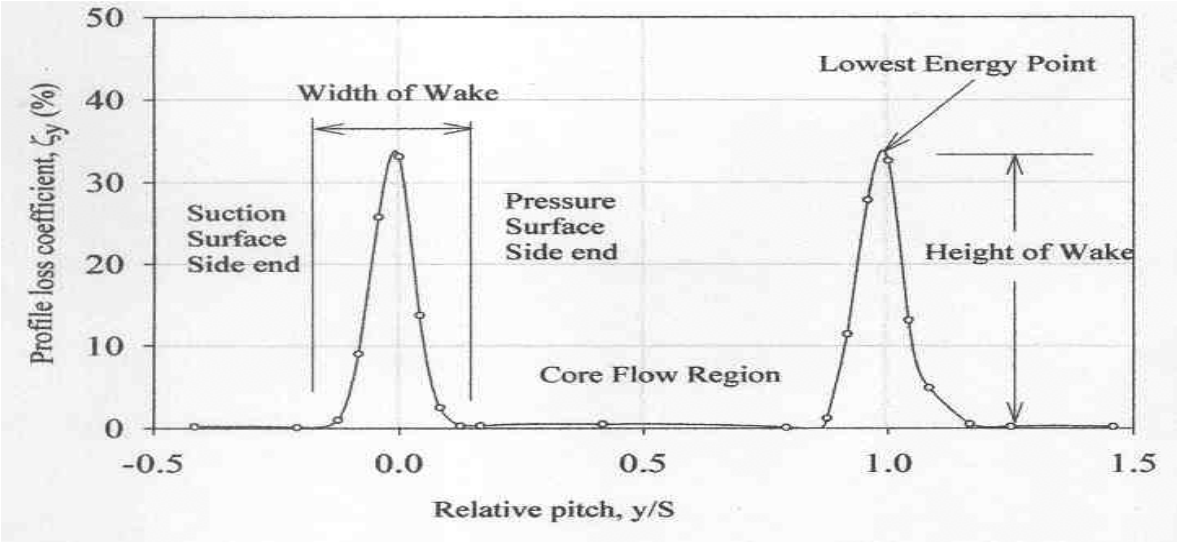

Fig. 4.1: Profile loss co-efficient verses relative pitch (Samasher, 2002)

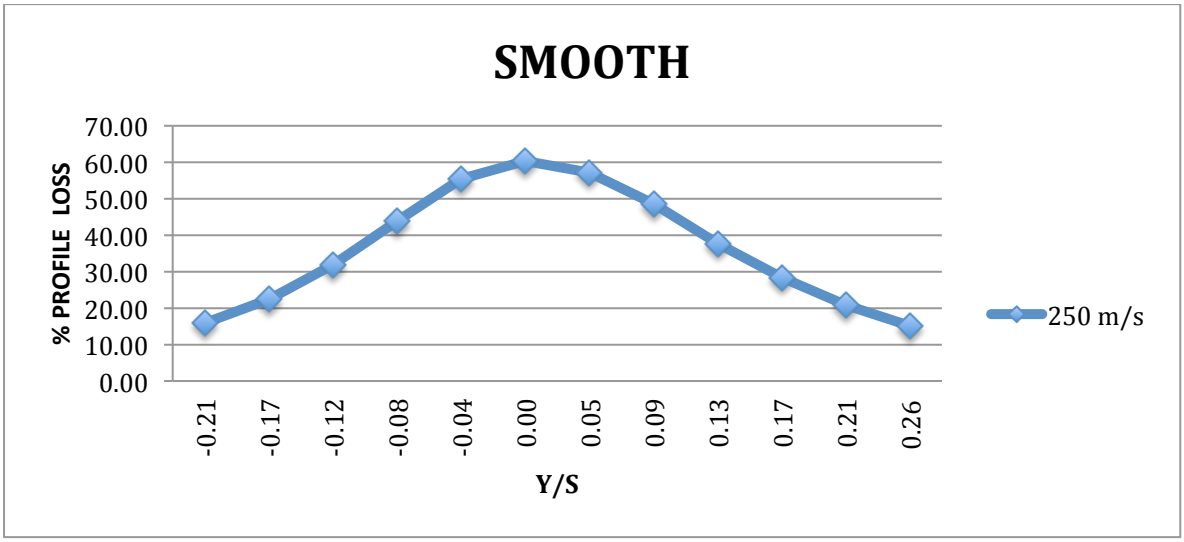

Fig. 4.2: Present Profile loss co-efficient verses relative pitch

The trend of computational results and the experimental data are similar. The pattern of variation of % profile loss co-efficient v/s non-dimensional pitch obtained by simulation and by the experimental results is similar. Hence this computational model is validated against the experimental results of Samsher [2002] and can be used for further work. Results validation are in Table 4.1.

This work is also validated against the experimental work of Seung Chul Back [8] and Leip old et al [9].

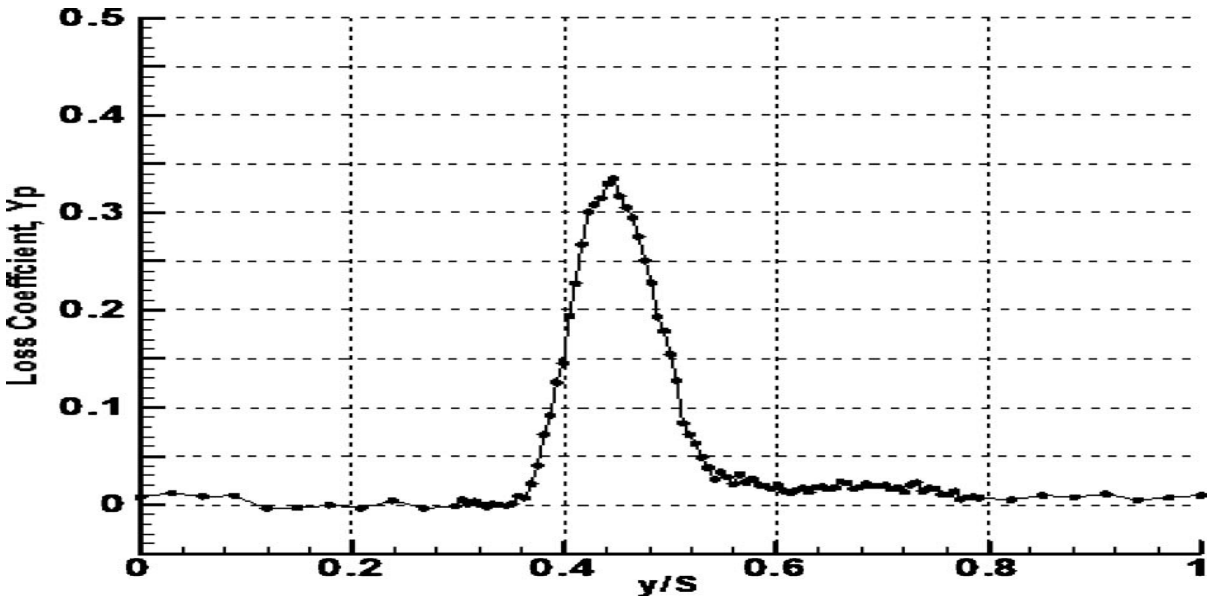

Fig. 4.3 Loss coefficient distribution of smooth blade at 0.3 chord downstream

Table 4.1: Comparison of Profile loss data for smooth blade

	x/c	Averaged profile loss
Present	0.4	32.57%
Seung chul back[8]	0.3	30 %
Leip old et al [9]	0.55	36%

The local roughness given on the suction and pressure surfaces of the blades are validated against used turbine blade in real life situation as shown in pictures from Fig. 4.4 To Fig. 4.5

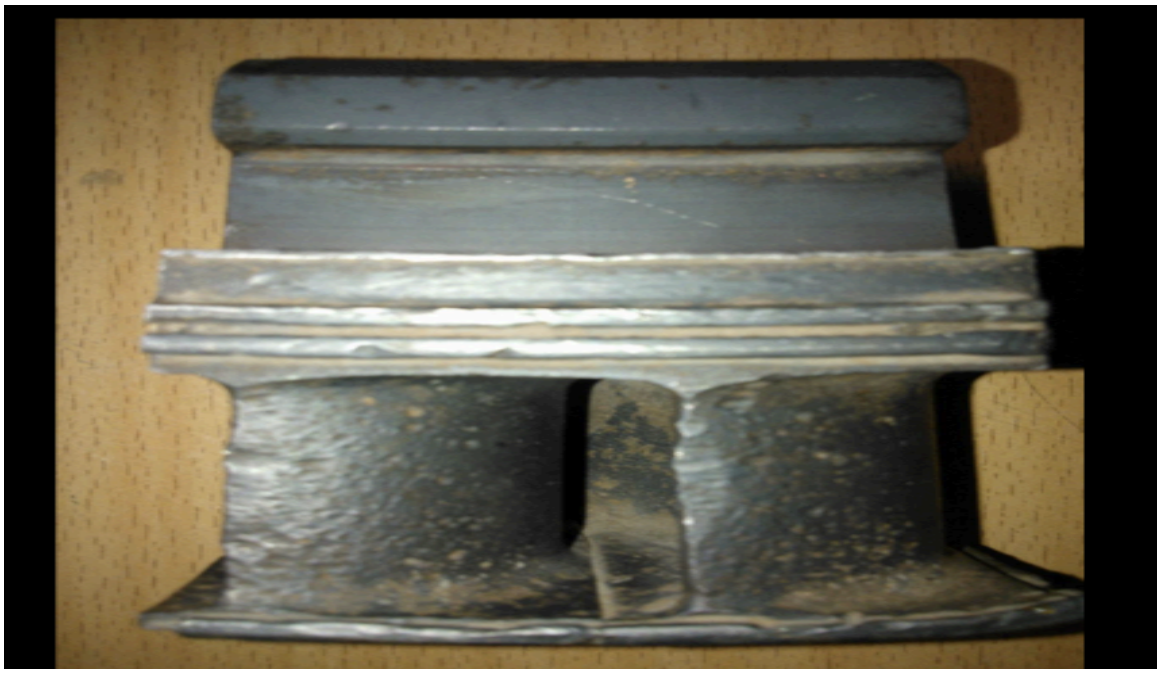

Fig. 4.4: Suction surface of blade

Fig. 4.5: Pressure surface of blade

4.2 Profile loss for smooth blades

From the Figure 4.6 the percentages profile loss of smooth blades for the inlet velocities 250 m/s, 300 m/s, and 350 m/s are 36.46 %, 35.21 % and 33.90 % respectively.

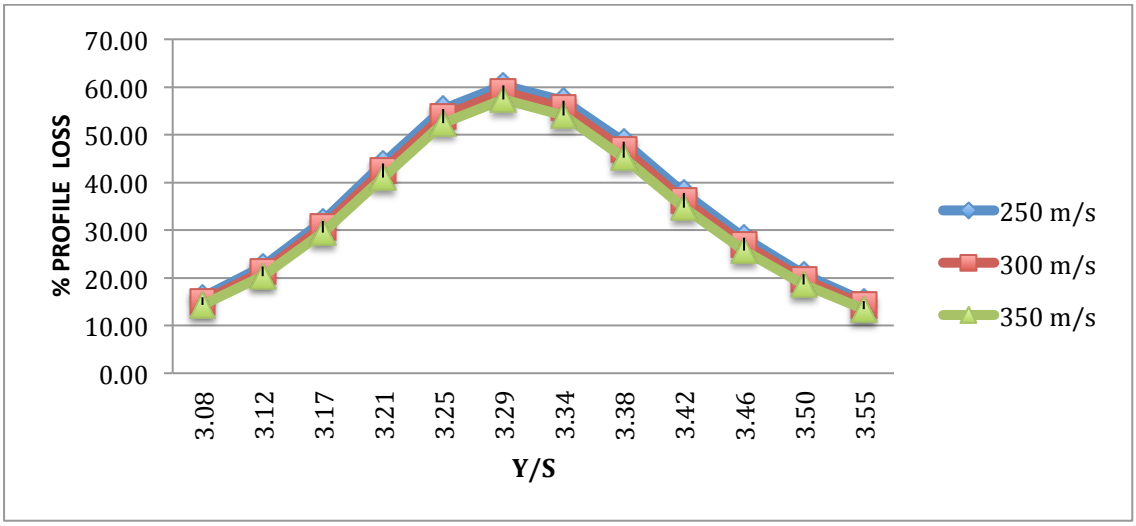

Fig 4.6: Percentage profile loss Vs. Y/S for smooth blade

4.3 Profile loss for both side rough blades

4.3.1 Profile loss for both side rough blades with roughness 300µm

Roughness is applied on the both side of the blades of Cascade and all other boundary conditions and location of measurement plane remained unchanged. From the Figure 4.7 the percentage profile loss of both side rough blades with roughness 300µm for the inlet velocities 250 m/s, 300 m/s, and 350 m/s are 37.0285 %, 35.7663 % and 34.4406 % respectively.

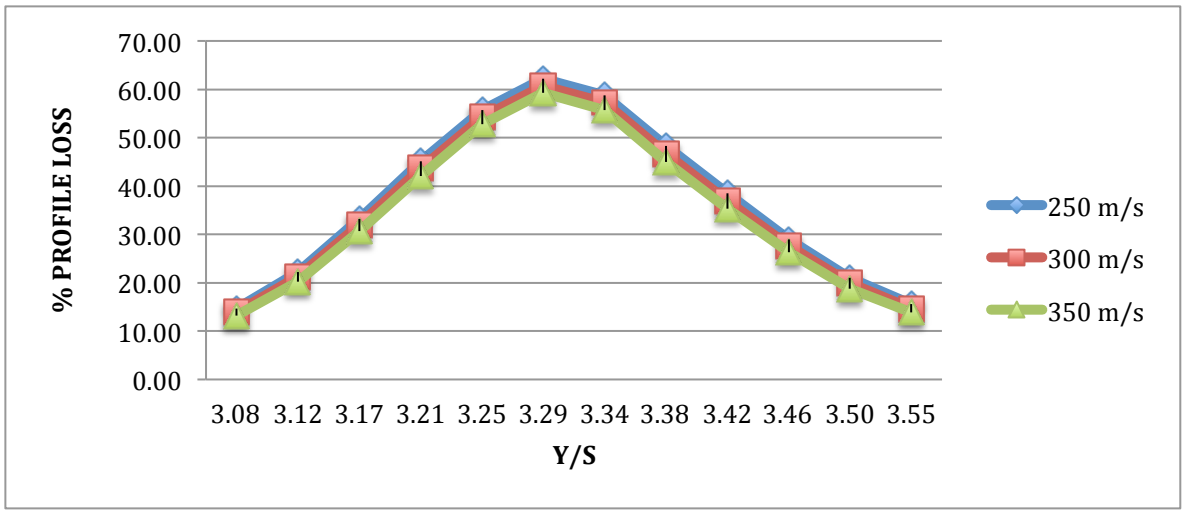

Fig 4.7: Percentage Profile loss Vs. Y/S for blade having roughness=300µm

4.3.2 Profile loss for both side rough blades with roughness 500µm

From the Figure 4.8 the percentage profile loss of both side rough blades with roughness 500µm for the inlet velocities 250 m/s, 300 m/s, and 350 m/s are 37.0285 %, 35.7663 % and 34.4406 % respectively.

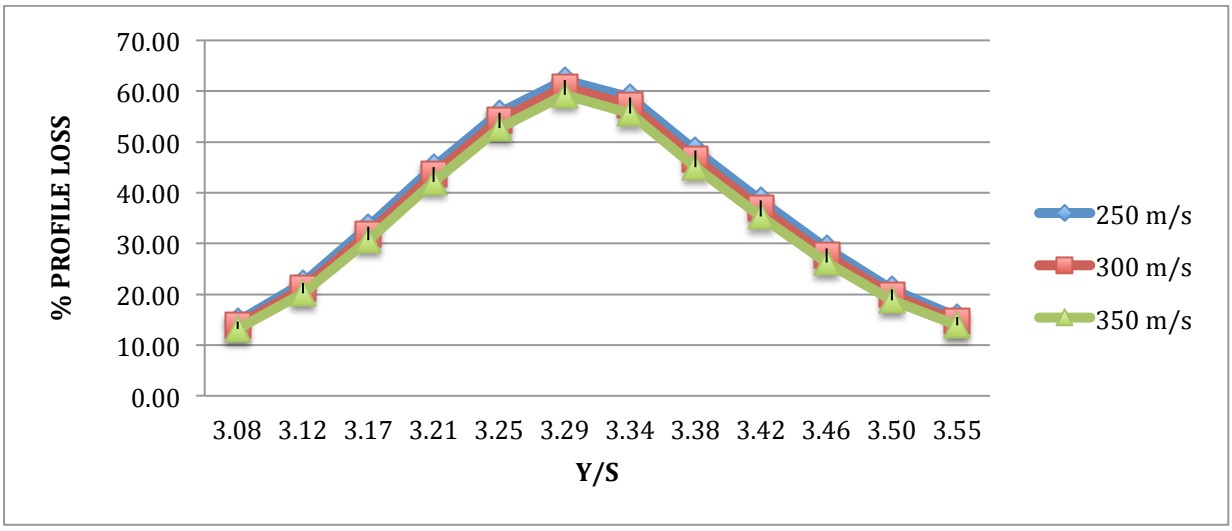

Fig 4.8: Percentage Profile loss Vs. Y/S for blade having roughness=500µm

4.3.3 Profile loss for both side rough blades with roughness 750µm

From the Figure 4.9 the percentage profile loss of both side rough blades with roughness 750µm for the inlet velocities 250 m/s, 300 m/s, and 350 m/s are 37.0287 %, 35.7661 % and 34.4406 % respectively.

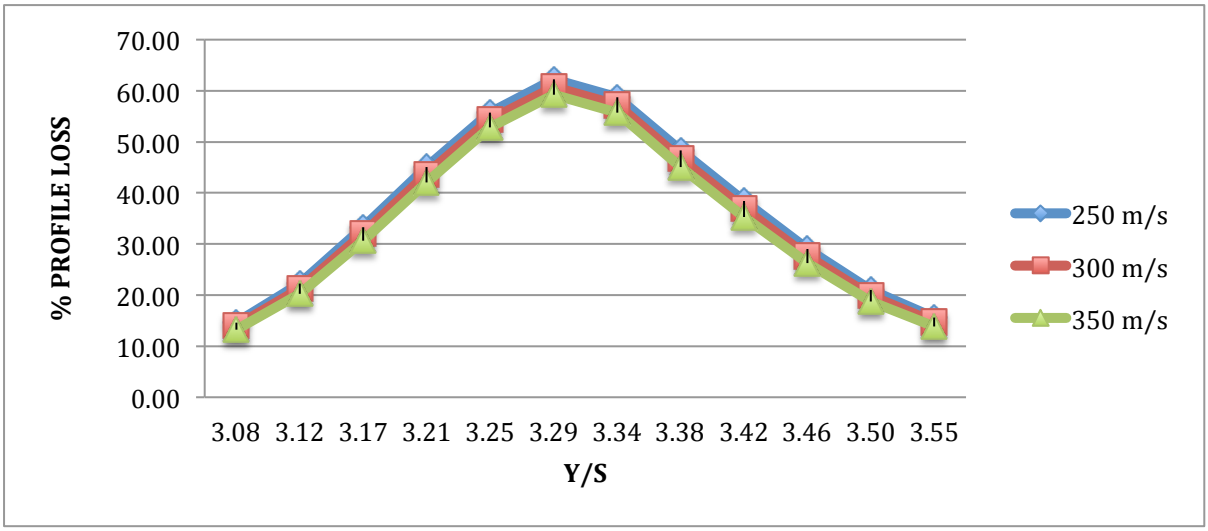

Fig 4.9: Percentage Profile loss Vs. Y/S for blade having roughness=750µm

4.4 Profile loss for rough suction surface

4.4.1 Profile loss for rough suction surface of blades with roughness 300µm

Roughness is applied only on the suction surface of the blades and all other boundary conditions and location of measurement plane remained unchanged. From the Figure 4.10 the percentage profile loss for rough suction surface with roughness 300µm for inlet velocities 250 m/s, 300 m/s, and 350 m/s are 37.0287 %, 35.7662 % and 34.4407 % respectively.

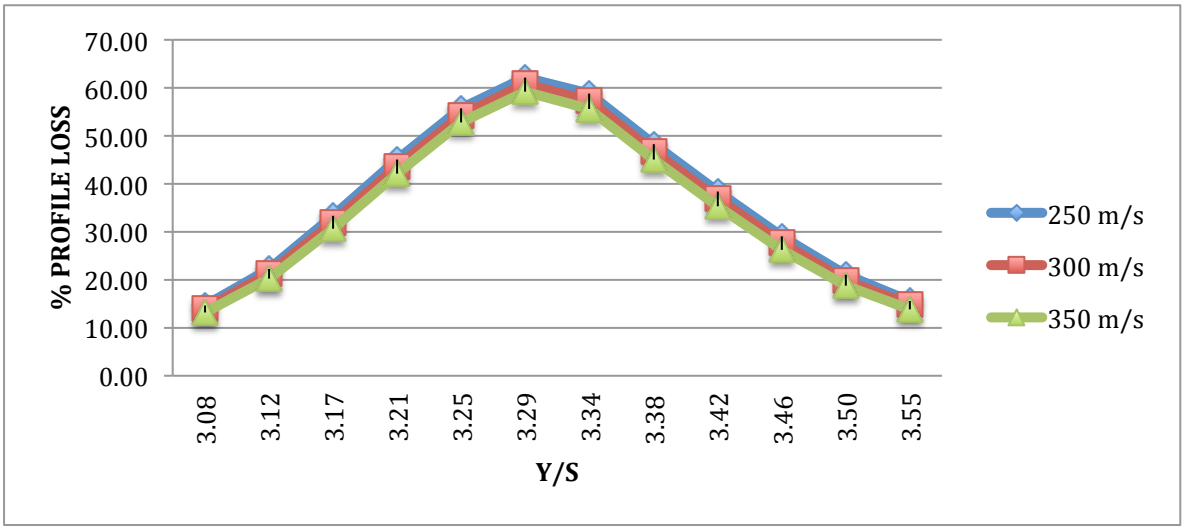

Fig 4.10: Percentage Profile loss Vs. Y/S for rough suction blade having roughness=300µm

4.4.2 Profile loss for rough suction surface of blade with roughness 500µm

From the Figure 4.11 the percentage profile loss for rough suction surface with roughness 500µm for inlet velocities 250 m/s, 300 m/s, and 350 m/s are 37.0284 %, 35.7663 % and 34.4408 % respectively.

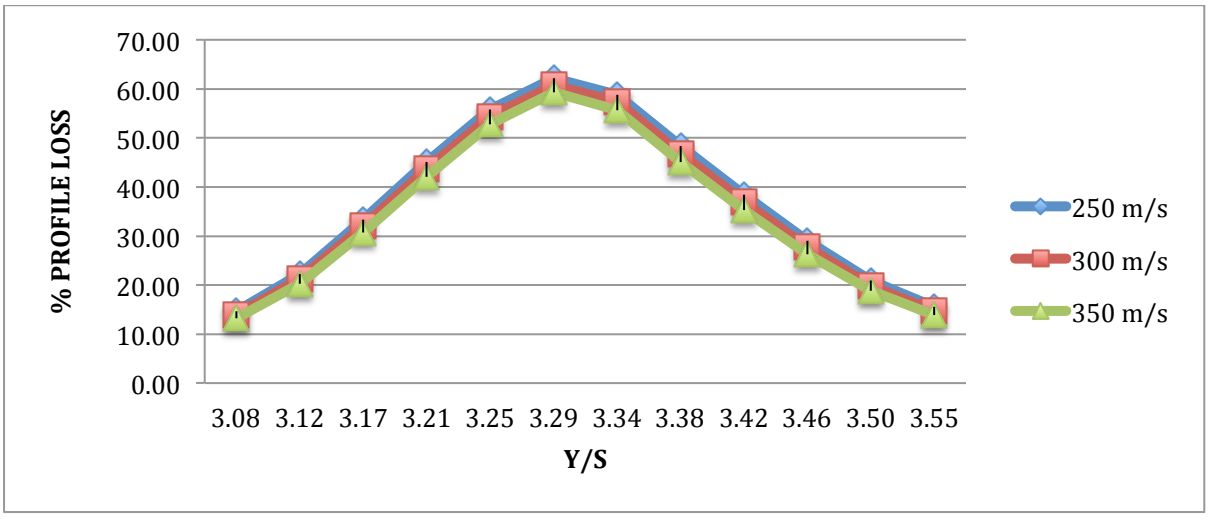

Fig 4.11:Percentage Profile loss Vs. Y/S for rough suction blade having roughness=500µm

4.4.3 Profile loss for rough suction surface of blades with roughness 750µm

From the Figure 4.12 the percentage profile loss for rough suction surface with roughness 750µm for inlet velocities 250 m/s, 300 m/s, and 350 m/s are 37.0285 %, 35.7663 % and 34.4406 % respectively.

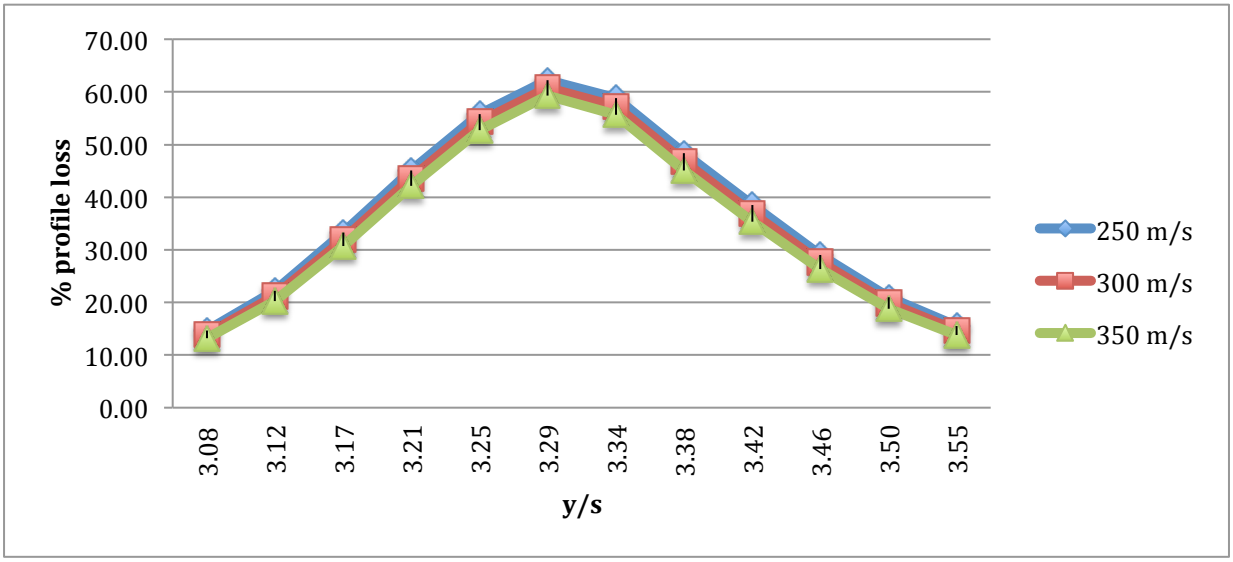

Fig 4.12: Percentage Profile loss Vs. Y/S for rough suction blade having roughness=750µm

4.5 Profile loss for rough pressure surface

4.5.1 Profile loss for rough pressure surface of blade with roughness 300µm

Roughness is applied only on the pressure surface of the blades and all other boundary conditions and location of measurement plane remained unchanged. From the Figure 4.13 the percentage profile loss for rough pressure surface with roughness 300µm for the inlet velocities 250 m/s, 300 m/s, and 350 m/s are 37.0284 %, 35.7663 % and 34.4407 % respectively.

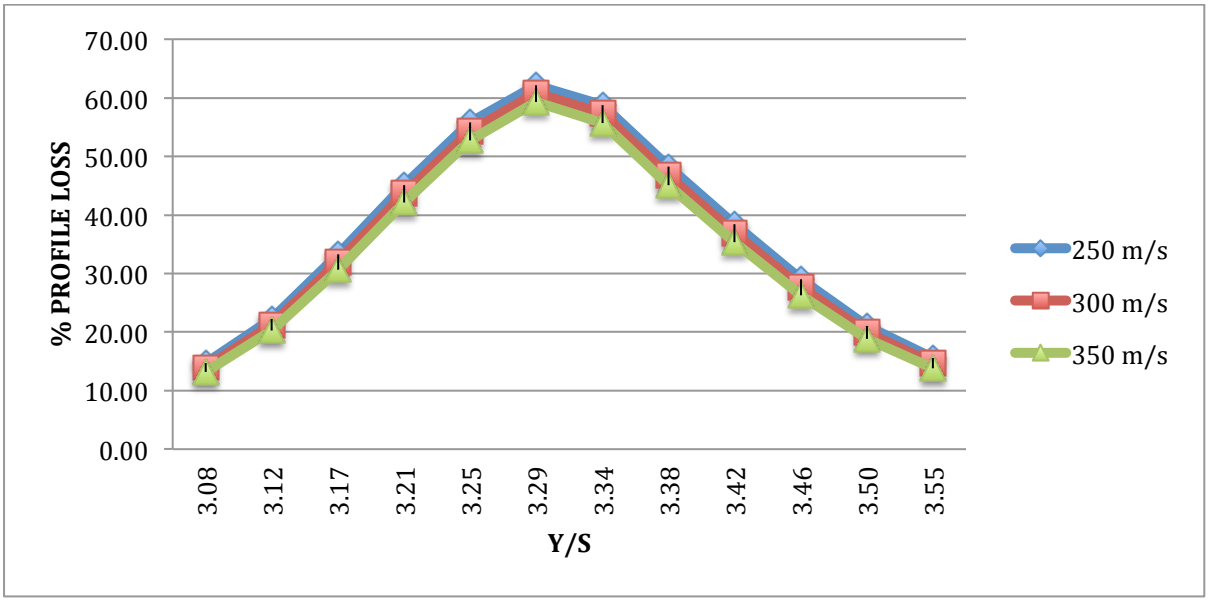

Fig 4.13: Percentage Profile loss Vs. Y/S for rough pressure blade having roughness=300µm

4.5.2 Profile loss for rough pressure surface of blades with roughness 500µm

From the Figure 4.14 the percentage profile loss for rough pressure surface with roughness 500µm for the inlet velocities 250 m/s, 300 m/s, and 350 m/s are 37.0284 %, 35.7663 % and 34.4409 % respectively.

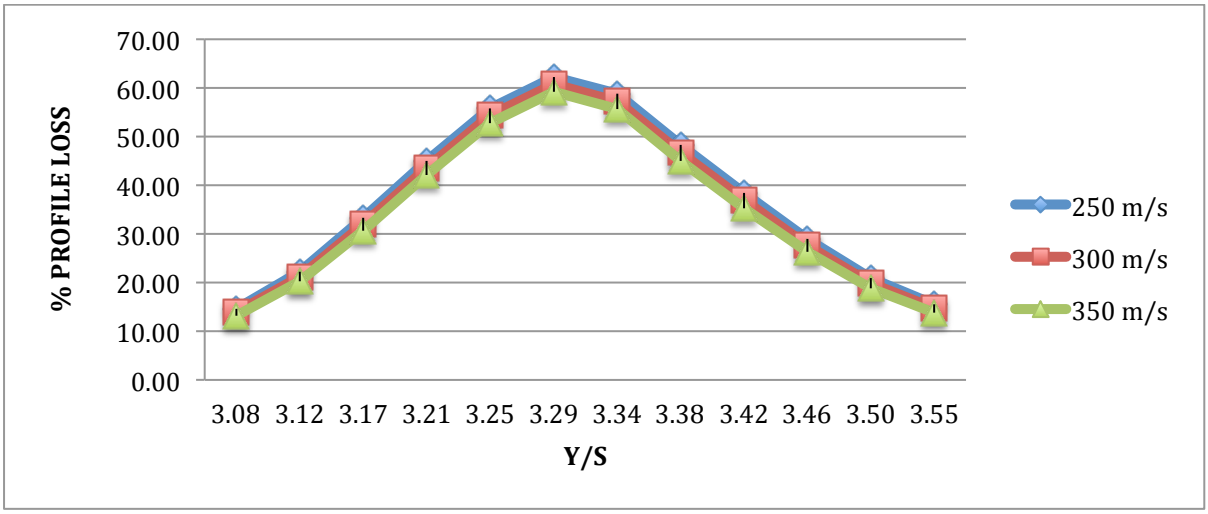

Fig 4.14: Percentage Profile loss Vs. Y/S for rough pressure blade having roughness=500µm

4.5.3 Profile loss for rough pressure surface of blade with roughness 750µm

From the Figure 4.15 the percentage profile loss for rough pressure surface with roughness 750µm for the inlet velocities 250 m/s, 300 m/s, and 350 m/s are 37.0287 %, 35.7663 % and 34.4408 % respectively.

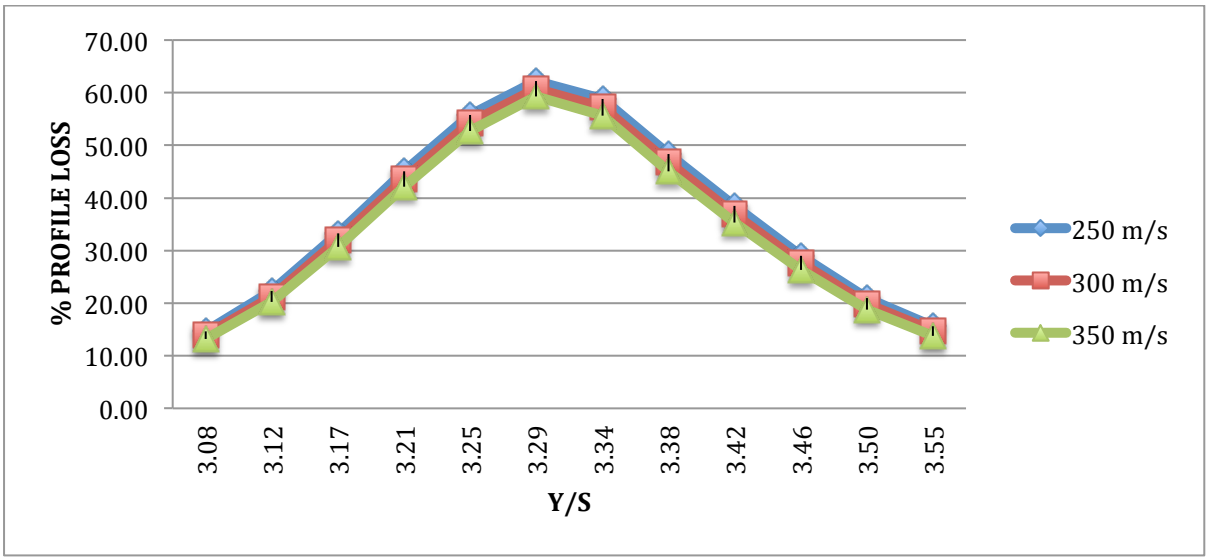

Fig 4.15: Percentage Profile loss Vs. Y/S for rough pressure blade having roughness=750µm

4.6 Profile loss for localized rough suction surface of blades

Suction surface of the blades of Cascade is divided into three equal parts. On the first section of the blade 300µm roughness is applied, on the second section of blade 500µm roughness is applied and on the third section of blade 750µm roughness is applied. All other boundary conditions and location of measurement plane remained unchanged.

From the Figure 4.16 the percentage profile loss for localized rough suction blade with inlet velocities 100 m/s, 250 m/s, 300 m/s, and 350 m/s are 52.1133 %, 50.1653 %, 56.2897 %, and 48.3466 % respectively.

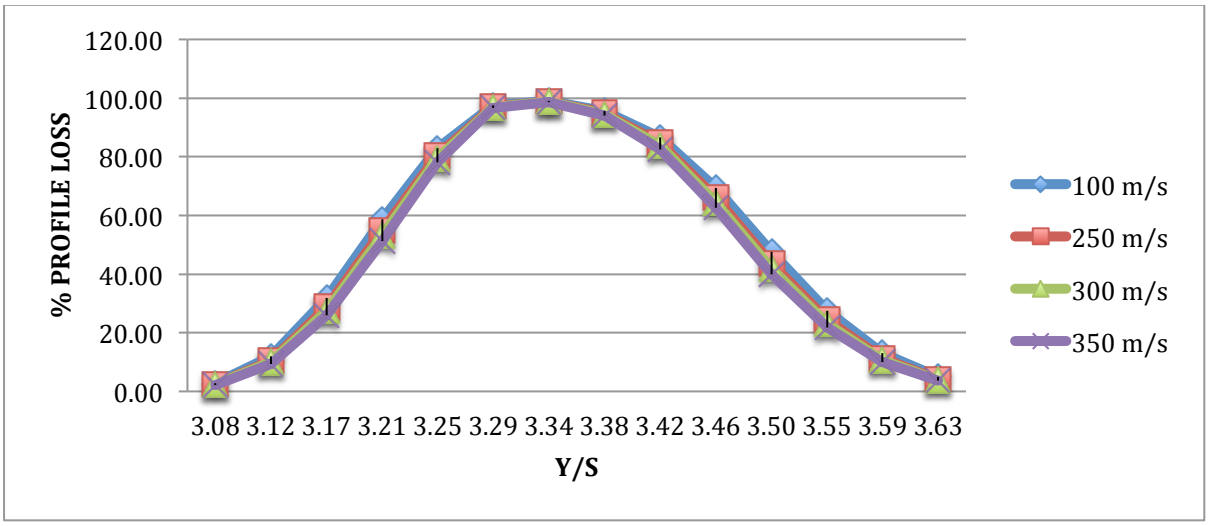

Fig 4.16: Percentage Profile loss Vs. Y/S for localized rough suction blade

4.7 Profile loss for localized rough pressure surface of blade

Pressure surface of the blades of Cascade is divided into three equal parts. On the first section of the blade 300µm roughness is applied, on the second section of blade 500µm roughness is applied and on the third section of blade 750µm roughness is applied. All other boundary conditions and location of measurement plane remained unchanged.

From the Figure 4.17 the percentage profile loss for localized rough pressure blade with inlet velocities 100 m/s, 250 m/s, 300 m/s, and 350 m/s are 52.3852 %, 50.4242 %, 49.5667 %, and 48.6000 % respectively.

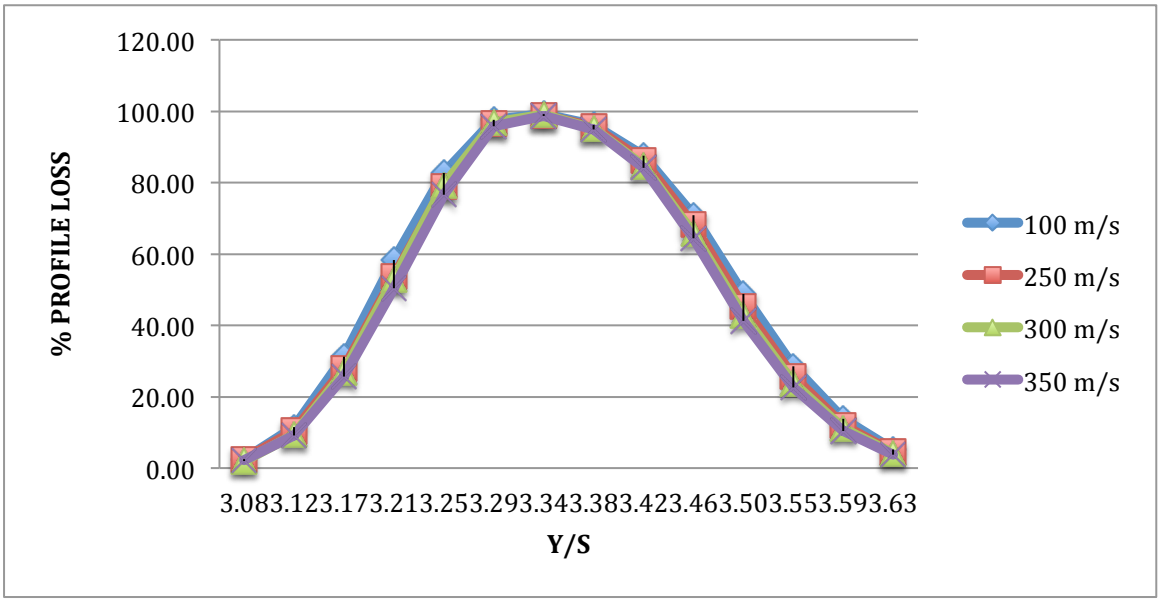

Fig 4.17: Percentage Profile loss Vs. Y/S for localized rough pressure blade

4.8 Flow Visualization

Contour plots of total pressure distribution for different cases

4.8.1: Smooth blades

4.8.1A: Inlet velocity 250 m/s.

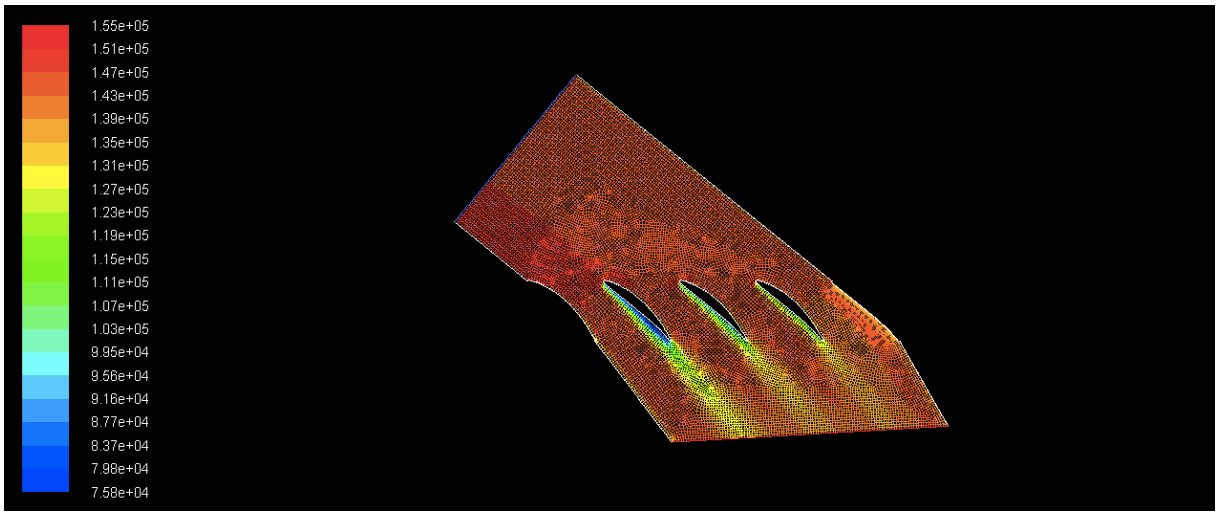

Fig. 4.18: Contour of total pressure for smooth blades for inlet velocity 250 m/s.

4.8.1B: Inlet velocity 300 m/s.

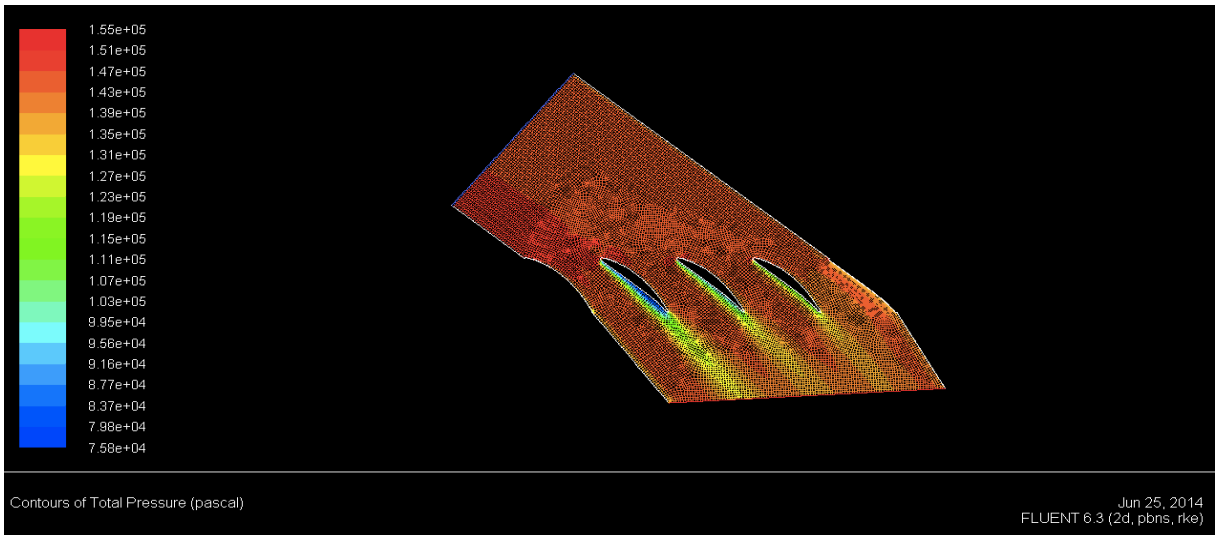

Fig 4.19: Contour of total pressure for smooth blades for inlet velocity 300 m/s.

4.8.1C: Inlet velocity 350 m/s.

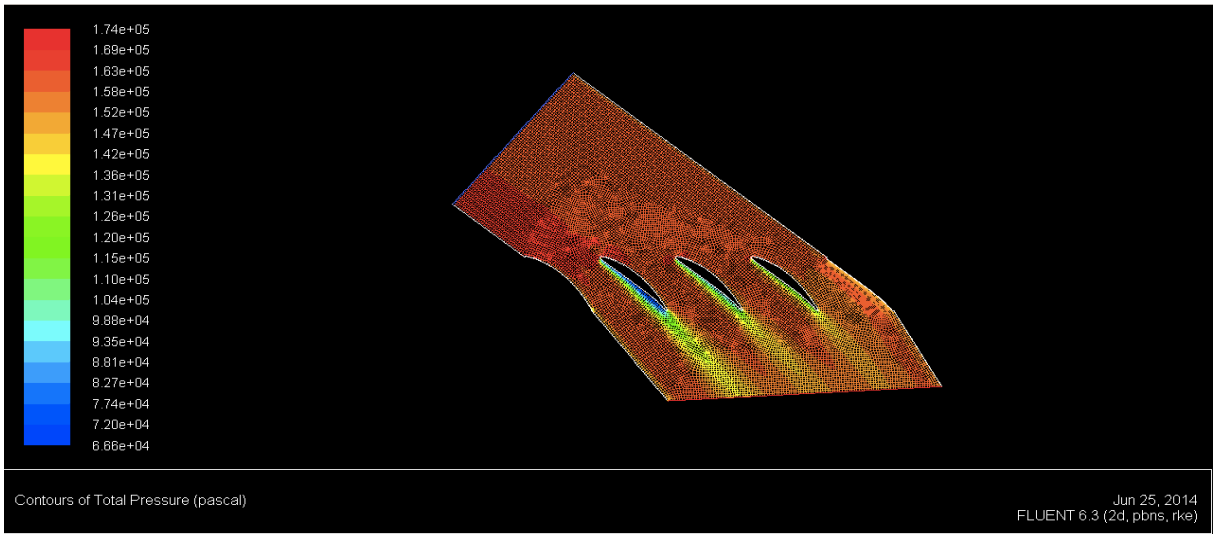

Fig 4.20: Contour of total pressure for smooth blades for inlet velocity 350 m/s

The various contours of total pressure are shown in Figures from Fig 4.18 to Fig 4.35. The red colored regions are the regions where the total pressure attains their

maximum values and the blue colored regions indicate the regions where the total pressure is at their minimum value.

At the inlet of the cascade total pressure drops due to expansion of fluid over the cascade. According to the obtained contour for the smooth blades in case of inlet velocity 250 m/s the total pressure changes from 7.58×10^4 Pa to 1.55×10^5 Pa and in case of inlet velocity 300 m/s the total pressure changes from 7.58×10^4 Pa to 1.55×10^5 Pa and in case of inlet velocity 350 m/s the total pressure changes from 6.66×10^4 Pa to 1.74×10^5 Pa. At the exit of cascade wakes are formed as shown in figs. 4.14.1 and total pressure drops. Pressure on the suction surface is more than the pressure surface. Total Pressure near to the pressure surface of the second blade is very less and increases as we move towards the blade along the non-dimensional distance Y/S. Wakes becomes narrower and near to the outlet boundary layer the wakes becomes wider and more diffused.

Profile loss is associated with the growth of boundary layer on the blade profile and the separation of the boundary layer occurs when the adverse pressure gradient on the surface or surface becomes too steep. The pressure gradient is more adverse at the mid span that is why the flow separation occurs at the mid span and profile losses are maximum.

Three boundary layer conditions of the cascade flow are:

1.Laminar separation, 2. Turbulent attached flow with hydraulically smooth blade surface, and 3. Turbulent attached flow with hydraulically rough blade surface.

From the Table 4.1 to Table 4.12 when the inlet velocity for the smooth blades is increases from 250 m/s to 350 m/s then Profile loss decreases by 7.02 %.

For the same velocity increases from 250 m/s to 350 m/s for the wholly rough blades having roughness 300µm, 500µm and 750µm Profile loss decreases by 6.988 %, 6.99 %, and 6.989 % respectively.

For the only rough suction surface having roughness 300µm, 500µm, and 750µm Profile loss for the increased velocity from 250 m/s to 350 m/s decreases by 6.989 %, 6.988 %, and 6.988 % respectively.

For the only rough pressure surface having roughness 300µm, 500µm, and 750µm Profile loss for the increased velocity from 250 m/s to 350 m/s decreases by 6.988 %, 6.987 %, and 6.988 % respectively.

In many cases the blades are attacked by dirt, corrosion and erosion during operation and causes non-uniform roughness on the blade surfaces.

For the localized rough suction surface having roughness 300µm, 500µm and 750µm decrease in Profile loss for the increase in inlet velocity from 250 m/s to 350 m/s is 3.625 %.

For the localized rough pressure surface having roughness 300µm, 500µm and 750µm decrease in Profile loss for the increase in inlet velocity from 250 m/s to 350 m/s is 3.617 %.

Profile loss decreases more rapidly in case of localized rough surfaces. Profile loss in case of localized roughness is about just half as compared with smooth blades and whole surface rough blades.

The inlet velocities are within the critical limit and the flow is within the hydraulic layer where the roughness and the location of roughness on the blade surface do not affect the profile loss very much. The conversion of energy in an axial compressor is influenced in great measure by the surface quality of the blading. For the low flow losses, the roughness values of the blade surface must be below certain limits.

Results show that within a limit Profile loss much not affected by the increase in inlet velocity significantly.

The contours for the other cases are shown in Figures from Fig. 4.12.2 to Fig. 4.12.6.

4.8.2: Wholly rough blades having roughness 300µm

4.8.2A: Inlet velocity 250 m/s.

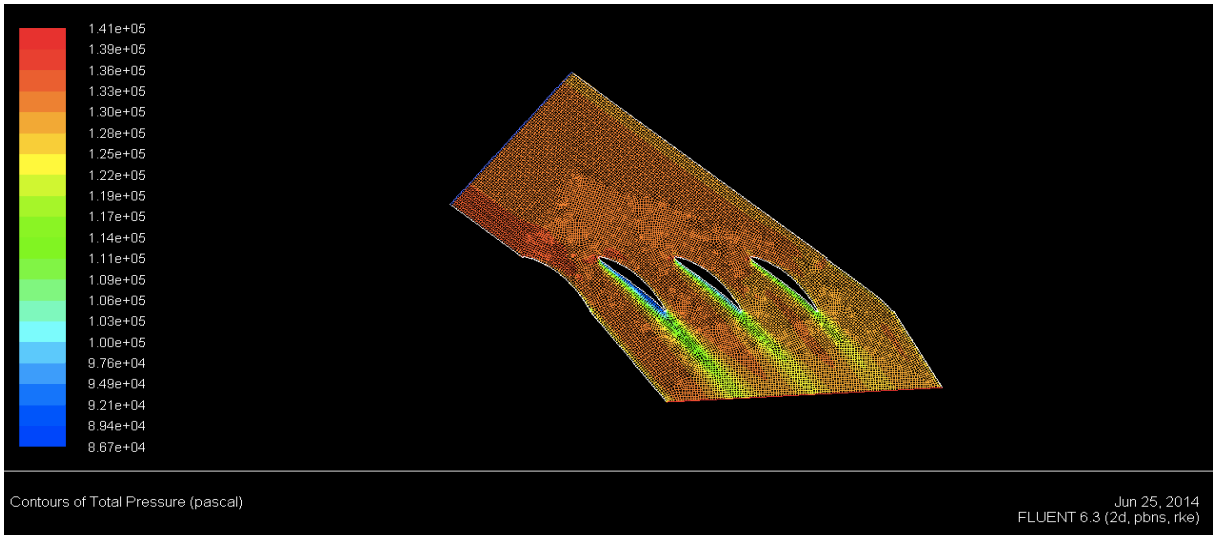

Fig 4.21: Contour of total pressure for wholly rough blades having roughness 300µm(VEL=250m/s)

4.8.2B: Inlet velocity 300 m/s.

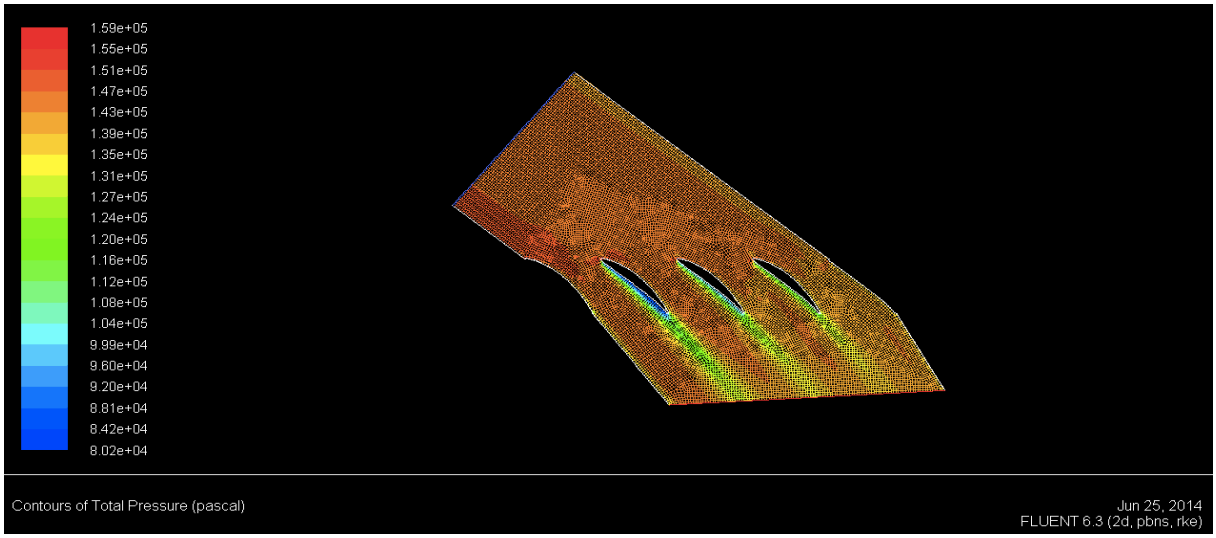

Fig 4.22: Contour of total pressure for wholly rough blades having roughness 300µm(VEL=300m/s)

4.8.2C: Inlet velocity 350 m/s.

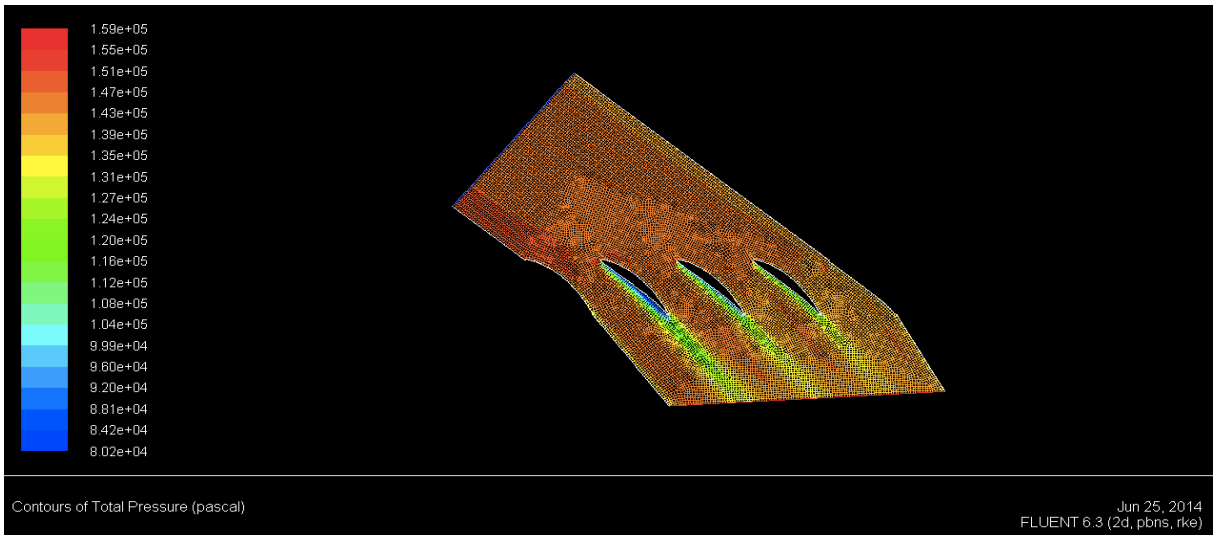

Fig 4.23: Contour of total pressure for wholly rough blades having roughness 300µm(VEL=350m/s)

4.8.3: rough suction surface of blades having roughness 300µm

4.8.3A: Inlet velocity 250 m/s.

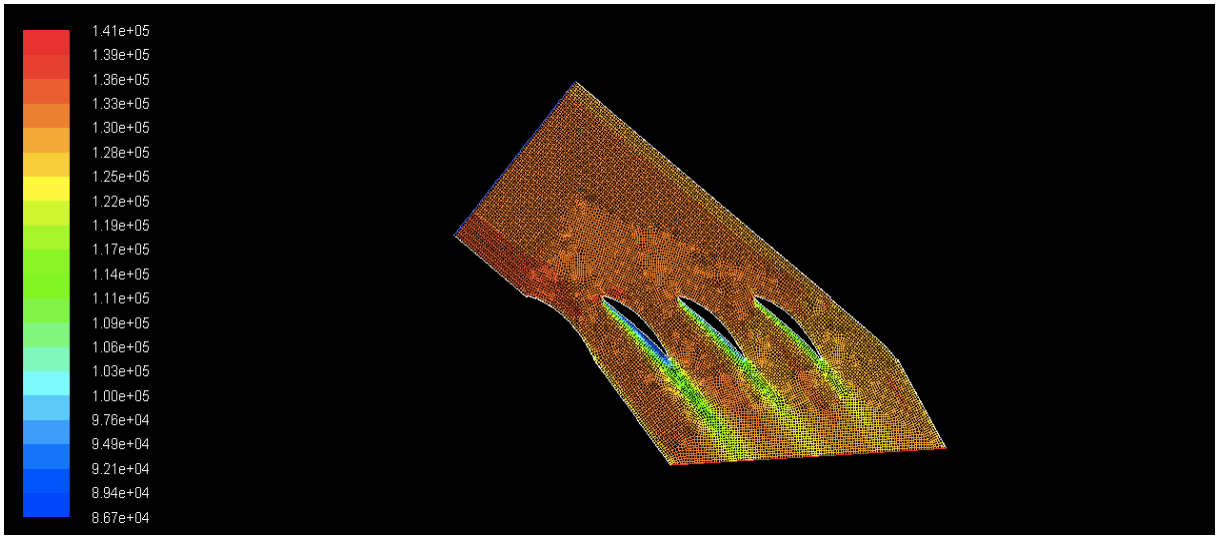

Fig 4.24:Contour of Total pressure for rough suction surface of blades having roughness 300µm(VEL=250 m/s)

4.8.3B: Inlet velocity 300 m/s.

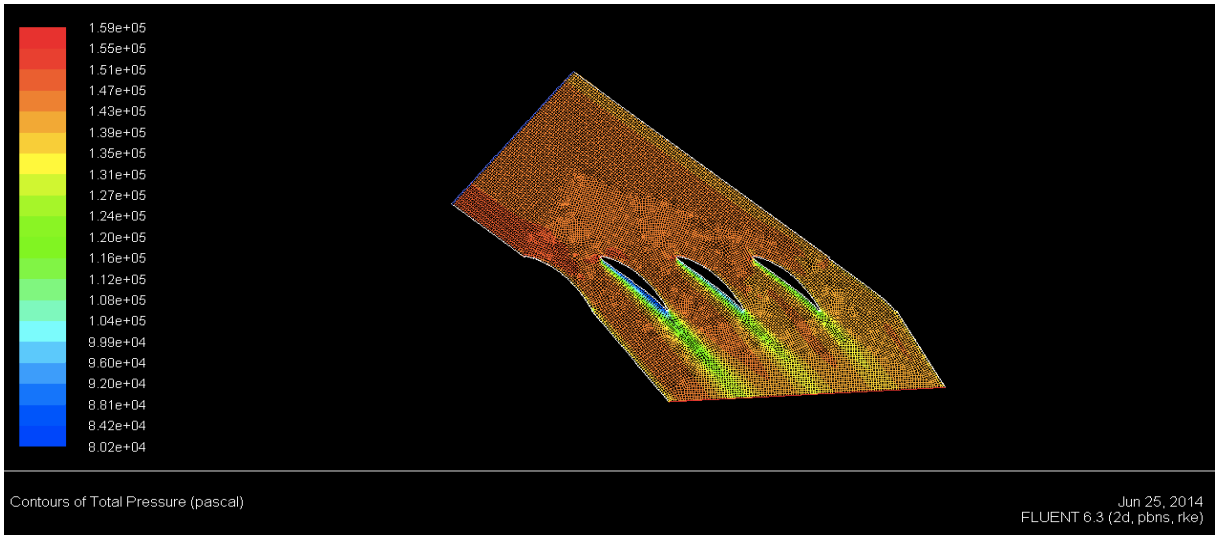

Fig 4.25:Contour of Total pressure for rough suction surface of blades having roughness 300µm(VEL=300 m/s)

4.8.3C: Inlet velocity 350 m/s.

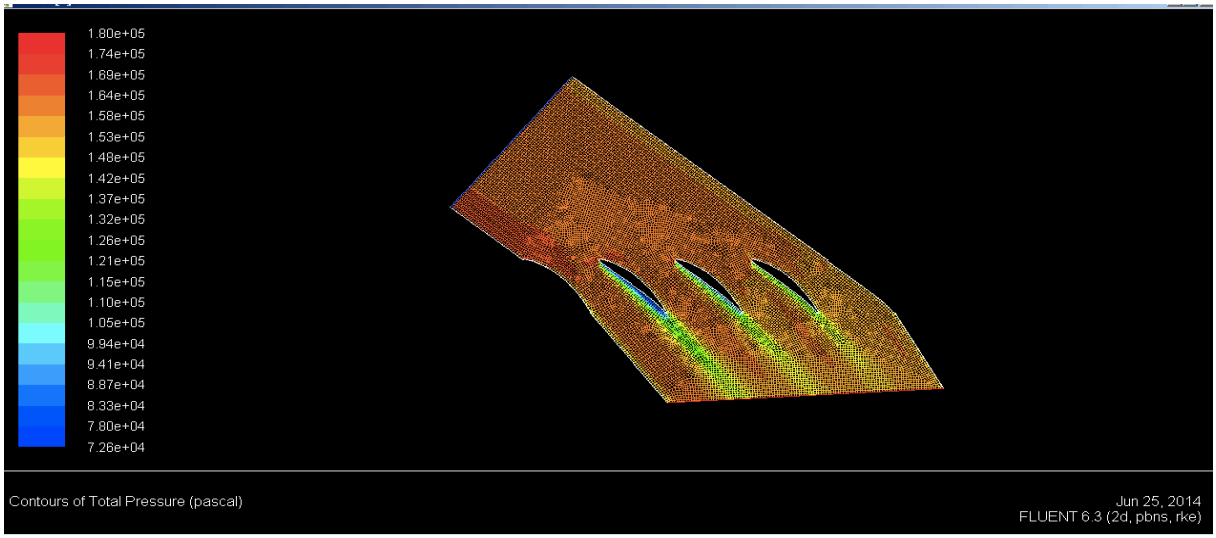

Fig 4.26:Contour of Total pressure for rough suction surface of blades having roughness 300µm(VEL=350 m/s)

4.8.4: Rough pressure surface of blades having roughness 300µm

4.8.4A: Inlet velocity 250 m/s.

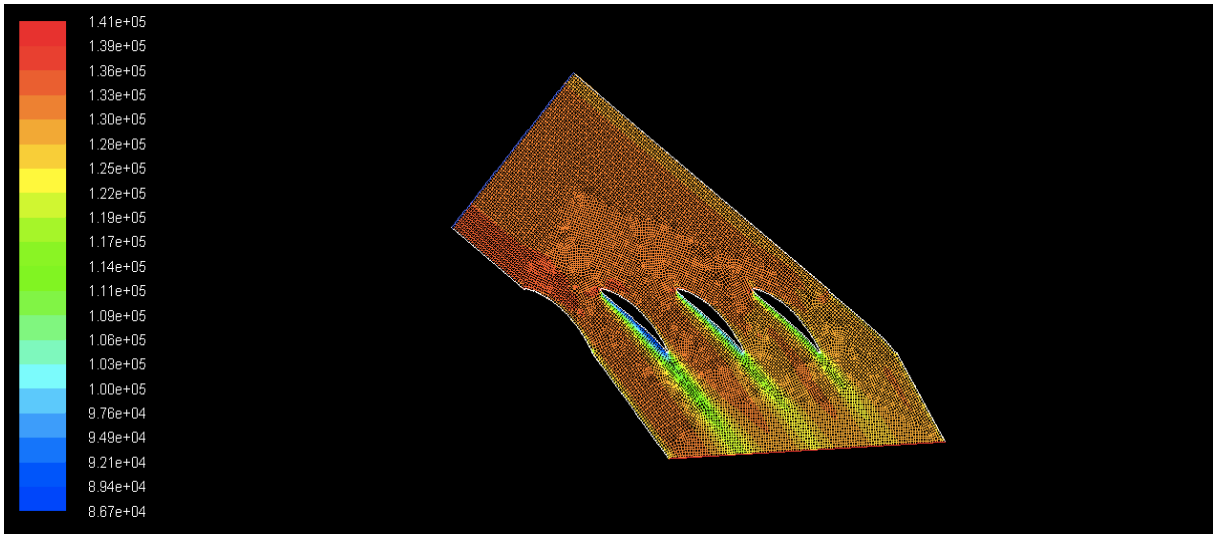

Fig 4.27: Contour of Total pressure for rough pressure surface of blades having roughness 300µm (VEL=250 m/s)

4.8.4B: Inlet velocity 300 m/s.

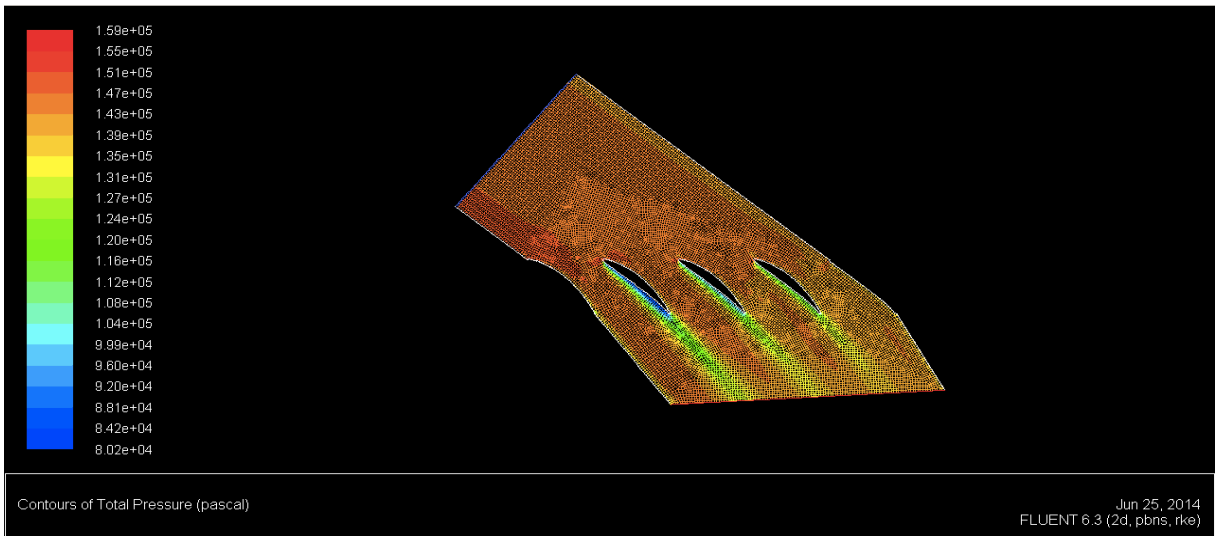

Fig 4.28: Contour of Total pressure for rough pressure surface of blades having roughness 300µm (VEL=300 m/s)

4.8.4C: Inlet velocity 350 m/s.

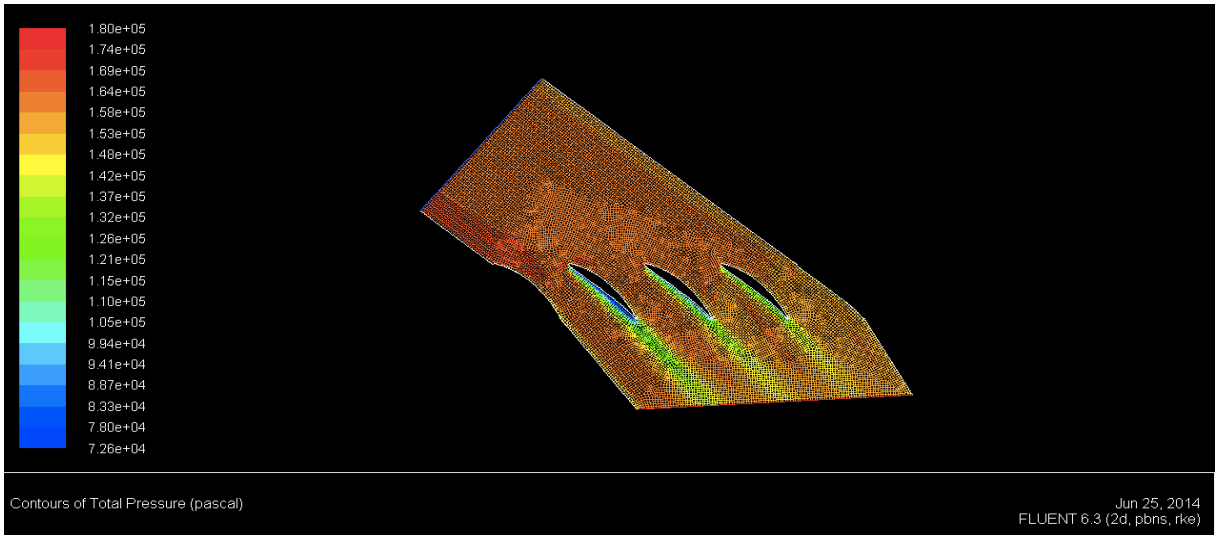

Fig 4.29: Contour of Total pressure for rough pressure surface of blades having roughness 300µm (VEL=350 m/s)

4.8.5: Localized rough suction surface of blades

4.8.5A: Inlet velocity 250 m/s.

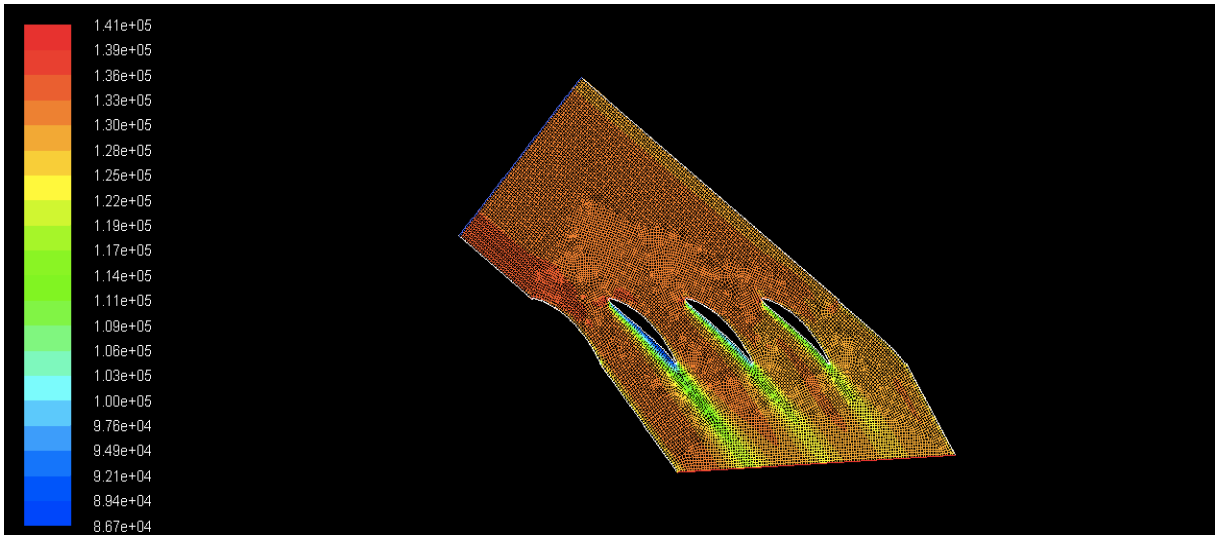

Fig 4.30: Contour of total pressure for localized rough suction surface of blades (VEL=250 m/s)

4.8.5B: Inlet velocity 300 m/s.

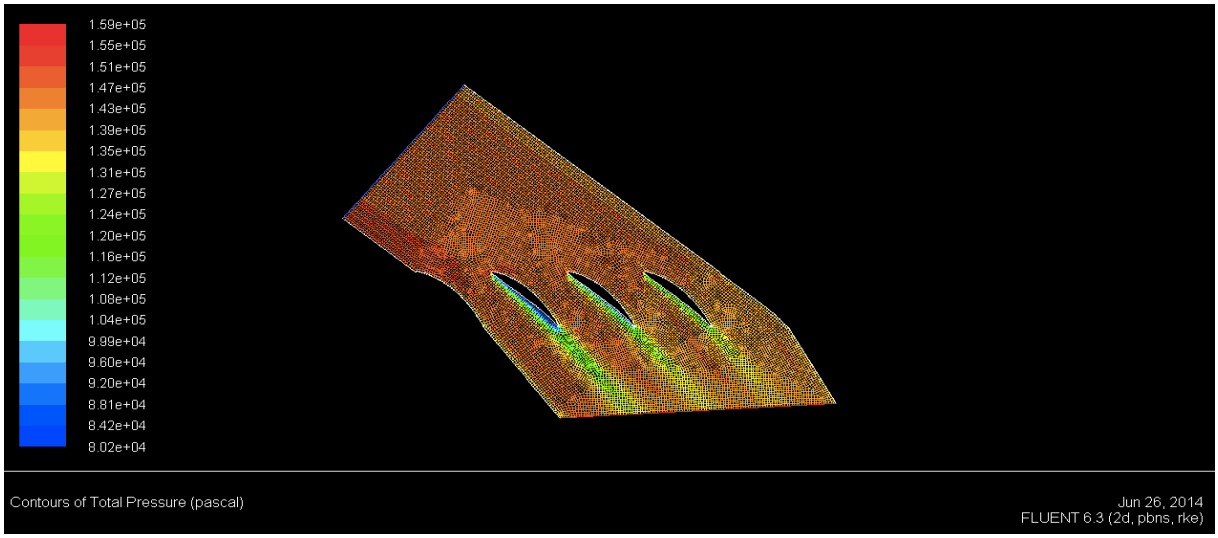

Fig 4.31: Contour of total pressure for localized rough suction surface of blades (VEL=300 m/s)

4.8.5C: Inlet velocity 350 m/s.

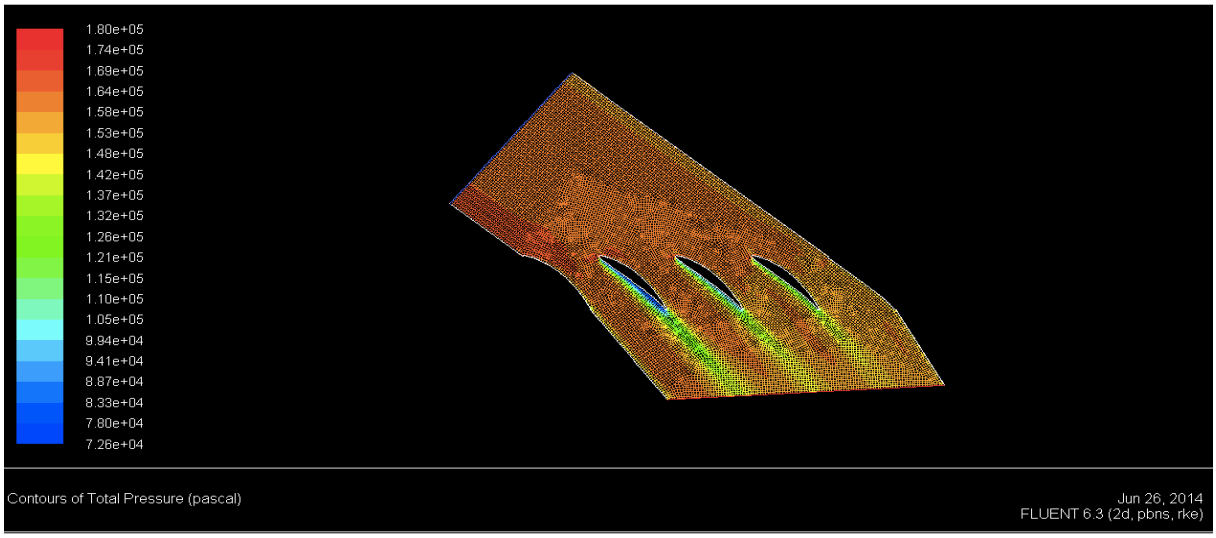

Fig 4.32: Contour of total pressure for localized rough suction surface of blades (VEL=350 m/s)

4.8.6: Localized rough pressure surface of blades

4.8.6A: Inlet velocity 250 m/s.

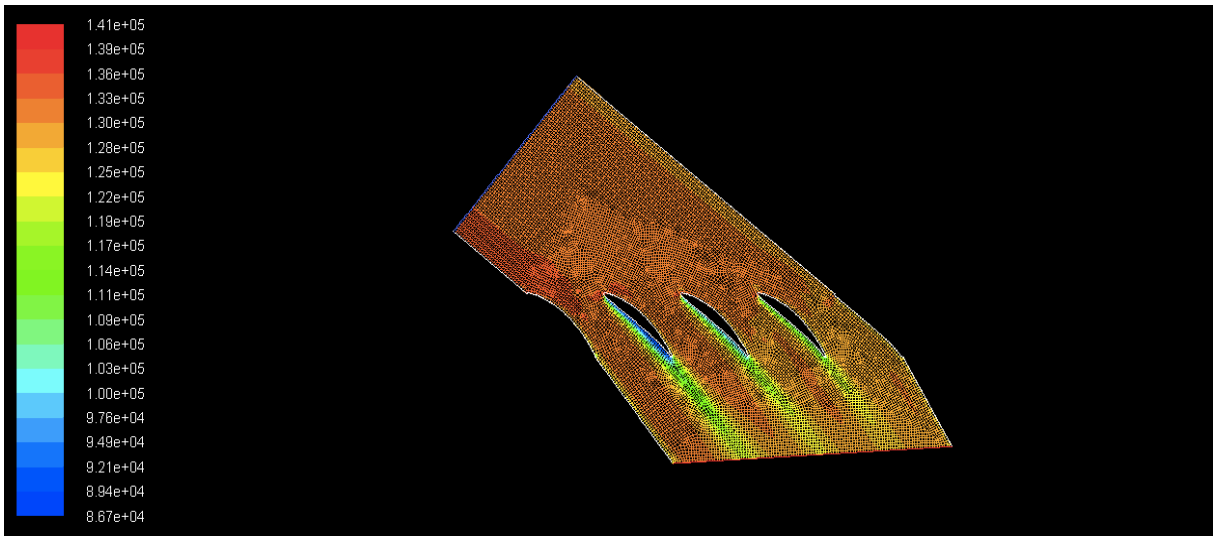

Fig 4.33: Contour of total pressure for localized rough pressure surface of blades (VEL=250 m/s)

4.8.6B: Inlet velocity 300 m/s.

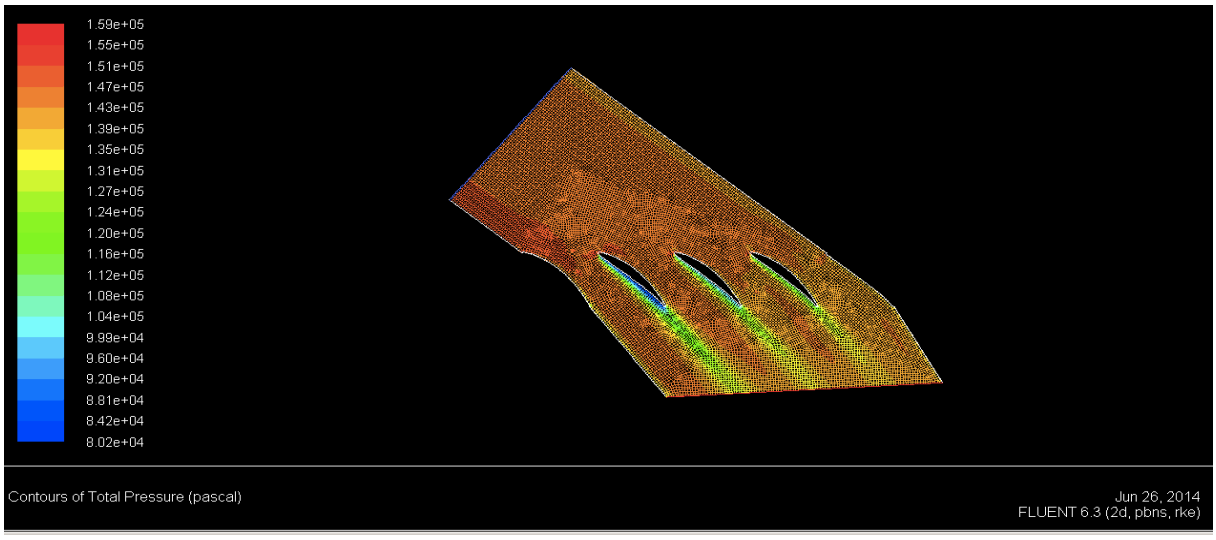

Fig 4.34: Contour of total pressure for localized rough suction surface of blades (VEL=300 m/s)

4.8.6C: Inlet velocity 350 m/s.

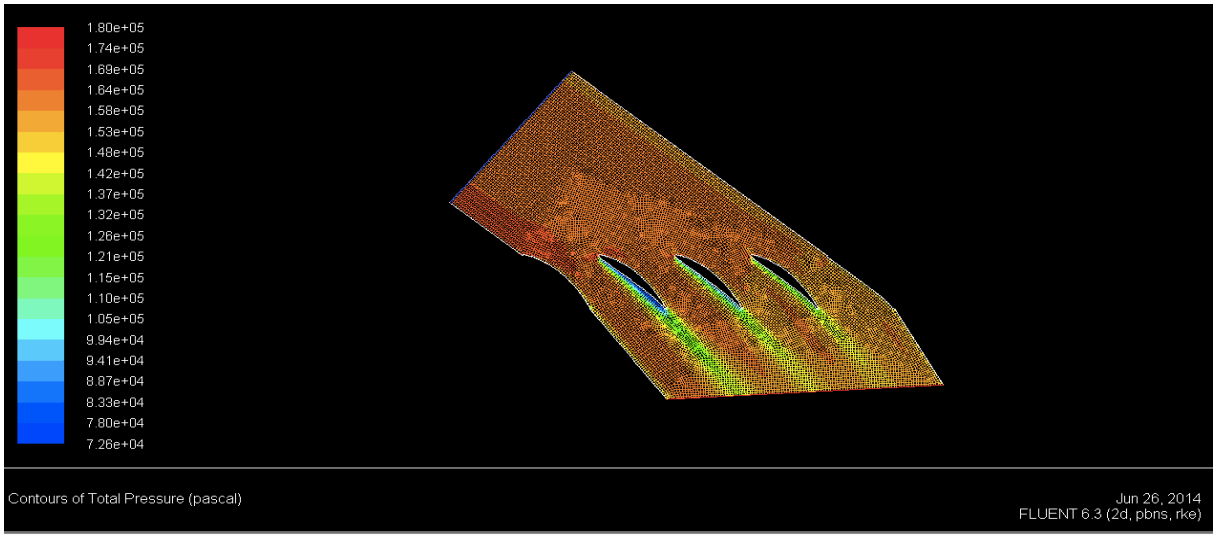

Fig 4.35: Contour of total pressure for localized rough suction surface of blades (VEL=350 m/s)

CHAPTER-5
CONCLUSION

It is concluded from the computational study of the effect of blade roughness that with the increase of inlet velocity Profile loss co-efficient decreases.

It is observed that for the smooth blades Profile loss co-efficient decreased by 7.02 % with the increase of inlet velocity from 250 m/s to 350 m/s.

For the constant velocity increase for the wholly rough blades having roughness 300µm, 500µm, 750µm profile loss decreased approximately by 6.98 %.

For the localized rough blades Profile loss changes rapidly. For the localized rough suction and localized rough pressure surface profile losses decreased by 3.625 % and 3.617 % respectively. The reduction in Profile loss is approximately half as compared with the smooth and rough blades. With the increase in Inlet velocity for different roughness the change in profile loss is very less.

CHAPTER-6

FUTURE SCOPE

The effect of roughness on the profile loss with different inlet velocities 250 m/s, 300 m/s and 350 m/s is analyzed by applying roughnesses 300µm, 500µm and 750µm on the full blade surface and on suction and pressure surfaces individually and by applying local roughness on both the suction and pressure surfaces.

Further there is a large area that has to be investigated. Future work can be done in finding the critical inlet velocity and limit of roughness beyond which the profile loss is affected in a considerable manner with increase in the inlet velocity.

Future work can be done for the localized rough blade to find the upper critical Reynolds Number above, which the flow is out of the hydraulic layer and to find the effect on the compressor efficiency.

The present used Cascade model is in 2D, which is some far from the real life situation. A three dimensional model of the cascade will be able to simulate the flow conditions in a more effective and realistic manner.

The effect of localized roughness on secondary flow and losses can also be studied for the same Cascade.

CHAPTER-7
REFERENCES

[1] Yahah, S., M., 2002, "Turbines, Compressors and Fans" Tata McGraw-Hill, New Delhi, Pg. No. 225-259.

[2] Shao-Wen Chen , Shi-Jun Sun, Hao Xu, Song-Tao Wang, 2013,"Experimental study of the impact of hole-type suction on the flow characteristics in a high-load Compressor cascade with a clearance" Journal of Experimental Thermal and Fluid Science, 51,220-226.

[3] Ahmed N, Yilbas B.S, Budair M.O, 1998, "Computational study into the flow field developed around a cascade of NACA 0012 airfoils" Journal of Computer Methods in Applied Mechanics and Engineering, 167, 17-32.

[4] Guo Shuang, Chen Shaowen et al, 2010, "Effects of Boundary Layer Suction on Aerodynamic Performance in a High-load Compressor Cascade" Chinese Journal of Aeronautics 23, 179-186.

[5] Kumar Singoria, Samsher, 2013, "The Study of End Losses in a Three Dimensional Rectilinear Low Speed Axial Flow Compressor Cascade" International Journal of Emerging Technology and Advanced Engineering, Volume 3, Issue 11.

[6] Pandey K.M, Chakraborty S, Deb K, 2012 "CFD Analysis of Flow through Compressor Cascade" International Journal of Soft Computing and Engineering, Volume-2, Issue-1.

[7] Hamed, Tabakoff W, and Singh D, 1997, "Modeling of Compressor Performance Deterioration Due to Erosion" International Journal of Rotating Machinery, Vol. 4, No. 4, Pp. 243-248.

[8] Seung Chul Back, June Hyuk Sohn, 2010, "Impact of Surface Roughness on Compressor Cascade Performance" ASME journal of fluids engineering, Vol. 132 / 064502.

[9] Leipold R, Boese M, and Fottner L, 2000, "The Influence of Technical Surface Roughness Caused by Precision Forging on the Flow Around a Highly Loaded Compressor Cascade," ASME Journal Turbomach., 122(3), pp. 416-425.

[10] Zhao Xiaohu, LI Yinghong et al, 2011, "Numerical Investigation of Flow Separation Control on a Highly Loaded Compressor Cascade by Plasma Aerodynamic Actuation" Chinese Journal of Aeronautics 25, pp. 349-360.

[11] Chen W.L, Lien F.S, 1998, "Computational prediction of flow around highly loaded compressor cascade blades with non-linear eddy-viscosity models" International Journal of Heat and Fluid Flow 19, pp. 307-319.

[12] Jia Huixia, XI Guang et. al, 2005, "Effects of Deposition Models on Deposition and Performance Deterioration in Axial Compressor Cascade" Chinese Journal of Aeronautics 18(1), pp. 20-24.

[13] Zhao Xiaohu, LI Yinghong et. al, 2012, "Numerical Investigation of Flow Separation Control on a Highly Loaded Compressor Cascade by Plasma Aerodynamic Actuation" Chinese Journal of Aeronautics 25, 349-360.

[14] Koubogiannis D.G, Athanasiadis A.N, Giannakoglou K.C, 2003, "One- and two-equation turbulence models for the prediction of complex cascade flows using unstructured grids" Journal of Computers & Fluids 32, 403–430.

[15] Kallinderis, Ahn, 2005, "Incompressible Navier–Stokes method with general hybrid meshes" Journal of Computational Physics 210, 75–108.

[16] Bammert K, Sandsted H, 1980, "Measurement of Boundary layer development along a turbine blade with Rough Surfaces" Journal of Engineering for Power 102, 978-983.

[17] Jouini D.B, Sjolander S. A, 2001, "Aerodynamic Performance of a transonic turbine Cascade at off-design conditions" Journal of Turbo Machinery 123, 510-517.

[18] Bolcs A, Sari O, 1998, "Influence of deposit on the flow in a turbine Cascade" Journal of Turbo Machinery 110, 512-519.

[19] Zachos P. K., Grech N. et al, 2011, "Experimental and Numerical Investigation of a Compressor Cascade at Highly Negative Incidence" Engineering Applications of Computational Fluid Mechanics 5, 26

[20] Nicola Aldia, Mirko Morinib et al.,2014, "Numerical Analysis of the Effects of Surface Roughness Localization on the Performance of an Axial Compressor Stage" Energy Procedia, 1057 – 1066.

[21] Zhong Jingjun , Han Shaobing, 2013, "Effect of tip geometry and tip Clearance on aerodynamic performance of a linear compressor cascade" Chinese Journal of Aeronautics 26(3), 583-593.

[22] Sathiyalingam K, Thomas Renalds C. J., 2012, "Prediction and measurement of Pressure Distribution over a Compressor Blade through a Cascade studies" Procedia Engineering 38, 2657 – 2662.

APPENDIX

Table 4.1: Percentage Profile loss for smooth blade

Y/S	% PROFILE LOSS (SMOOTH)		
	VEL=250 m/s	VEL=300 m/s	VEL= 350 m/s
3.08	15.91	15.14	14.36
3.12	22.33	21.35	20.33
3.17	31.92	30.69	29.42
3.21	43.92	42.51	41.04
3.25	55.35	53.93	52.42
3.29	60.40	58.98	57.45
3.34	57.15	55.64	54.02
3.38	48.51	46.92	45.24
3.42	37.76	36.25	34.67
3.46	28.40	27.09	25.74
3.50	20.80	19.74	18.65
3.55	15.11	14.28	13.43
AVG	36.46	35.21	33.90

Table 4.2: Percentage Profile loss for both side rough (Roughness=300µm)

Y/S	% PROFILE LOSS (ROUGHNESS=300µm)		
	VEL=250 m/s	**VEL=300 m/s**	**VEL=350 m/s**
3.08	14.64	13.93	13.20
3.12	22.25	21.26	20.25
3.17	33.27	31.99	30.67
3.21	45.07	43.64	42.13
3.25	55.77	54.33	52.78
3.29	62.19	60.79	59.27
3.34	58.80	57.29	55.67
3.38	48.31	46.72	45.04
3.42	38.45	36.93	35.33
3.46	29.02	27.68	26.30
3.50	20.98	19.91	18.81
3.55	15.57	14.71	13.84
AVG	37.0285	35.7663	34.4406

Table 4.3: Percentage Profile loss for both side rough (Roughness=500µm)

Y/S	% PROFILE LOSS (ROUGHNESS=500µm)		
	VEL= 250 m/s	VEL= 300 m/s	VEL=350 m/s
3.08	14.64	13.92	13.19
3.12	22.24	21.26	20.25
3.17	33.27	31.99	30.66
3.21	45.07	43.63	42.12
3.25	55.77	54.32	52.78
3.29	62.19	60.78	59.26
3.34	58.79	57.29	55.67
3.38	48.31	46.72	45.03
3.42	38.45	36.93	35.33
3.46	29.01	27.68	26.29
3.50	20.98	19.91	18.80
3.55	15.57	14.71	13.84
AVG	37.0285	35.7663	34.44

Table 4.4: Percentage Profile loss for both side rough (Roughness=750µm)

Y/S	% PROFILE LOSS (ROUGHNESS=750µm)		
	VEL= 250 m/s	VEL= 300 m/s	VEL= 350 m/s
3.08	14.64	13.92	13.19
3.12	22.24	21.26	20.25
3.16	33.27	31.99	30.66
3.20	45.07	43.63	42.12
3.25	55.77	54.32	52.78
3.29	62.19	60.78	59.26
3.33	58.79	57.29	55.67
3.37	48.31	46.72	45.03
3.41	38.45	36.93	35.33
3.46	29.01	27.68	26.29
3.50	20.98	19.91	18.80
3.55	15.57	14.71	13.84
AVG	37.0287	35.7661	34.4406

Table 4.5: Percentage Profile loss for rough suction surface (Roughness= 300µm)

Y/S	% PROFILE LOSS FOR ROUGH SUCTION (ROUGHNESS=300µm)		
	VEL=250 m/s	VEL=300 m/s	VEL=350 m/s
3.08	14.64	13.92	13.19
3.12	22.24	21.26	20.25
3.17	33.27	31.99	30.66
3.21	45.07	43.63	42.12
3.25	55.77	54.32	52.78
3.29	62.19	60.78	59.26
3.34	58.79	57.29	55.67
3.38	48.31	46.72	45.03
3.42	38.45	36.93	35.33
3.46	29.01	27.68	26.29
3.50	20.98	19.91	18.80
3.55	15.57	14.71	13.84
AVG	37.0287	35.7662	34.4407

Table 4.6: Percentage Profile loss for rough suction surface (Roughness=500µm)

Y/S	% PROFILE LOSS FOR ROUGH SUCTION (ROUGHNESS=500µm)		
	VEL=250 m/s	VEL=300 m/s	VEL=350 m/s
3.08	14.64	13.92	13.19
3.12	22.24	21.26	20.25
3.17	33.27	31.99	30.66
3.21	45.07	43.63	42.12
3.25	55.77	54.32	52.78
3.29	62.19	60.78	59.26
3.34	58.79	57.29	55.67
3.38	48.31	46.72	45.03
3.42	38.45	36.93	35.33
3.46	29.01	27.68	26.29
3.50	20.98	19.91	18.80
3.55	15.57	14.71	13.84
AVG	37.0284	35.7663	34.4408

Table 4.7: Percentage Profile loss for rough suction surface (Roughness= 750µm)

Y/S	% PROFILE LOSS FOR ROUGH SUCTION (ROUGHNESS=750µm)		
	VEL=250 m/s	VEL=300 m/s	VEL=350 m/s
3.08	14.64	13.92	13.19
3.12	22.25	21.26	20.25
3.17	33.27	31.99	30.66
3.21	45.07	43.63	42.12
3.25	55.77	54.32	52.78
3.29	62.19	60.78	59.26
3.34	58.79	57.29	55.67
3.38	48.31	46.72	45.03
3.42	38.45	36.93	35.33
3.46	29.01	27.68	26.29
3.50	20.98	19.91	18.80
3.55	15.57	14.71	13.84
AVG	37.0285	35.7663	34.4406

Table 4.8: Percentage Profile loss for rough pressure surface (Roughness= 300µm)

Y/S	% PROFILE LOSS FOR ROUGH PRESSURE (ROUGHNESS=300µm)		
	VEL=250 m/s	VEL=300 m/s	VEL=350 m/s
3.08	14.64	13.92	13.19
3.12	22.24	21.26	20.25
3.17	33.27	31.99	30.66
3.21	45.07	43.63	42.12
3.25	55.77	54.32	52.78
3.29	62.19	60.78	59.26
3.34	58.79	57.29	55.67
3.38	48.31	46.72	45.03
3.42	38.45	36.93	35.33
3.46	29.01	27.68	26.29
3.50	20.98	19.91	18.80
3.55	15.57	14.71	13.84
AVG	37.0284	35.7663	34.4407

Table 4.9: Percentage Profile loss for rough pressure surface (Roughness =500µm)

Y/S	% PROFILE LOSS FOR ROUGH PRESSURE (ROUGHNESS=500µm)		
	VEL=250 m/s	VEL=300 m/s	VEL=350 m/s
3.08	14.64	13.92	13.19
3.12	22.25	21.26	20.25
3.17	33.27	31.99	30.66
3.21	45.07	43.63	42.12
3.25	55.77	54.32	52.78
3.29	62.19	60.78	59.26
3.34	58.79	57.29	55.67
3.38	48.31	46.72	45.03
3.42	38.45	36.93	35.33
3.46	29.01	27.68	26.29
3.50	20.98	19.91	18.80
3.55	15.57	14.71	13.84
AVG	37.0284	35.7663	34.4409

Table 4.10: Percentage Profile loss for rough pressure surface (Roughness =750µm)

Y/S	% PROFILE LOSS FOR ROUGH PRESSURE (ROUGHNESS=750µm)		
	VEL = 250 m/s	VEL=300 m/s	VEL= 350 m/s
3.08	14.64	13.92	13.19
3.12	22.24	21.26	20.25
3.17	33.27	31.99	30.66
3.21	45.07	43.63	42.12
3.25	55.77	54.32	52.78
3.29	62.19	60.78	59.26
3.34	58.79	57.29	55.67
3.38	48.31	46.72	45.03
3.42	38.45	36.93	35.33
3.46	29.01	27.68	26.29
3.50	20.98	19.91	18.80
3.55	15.57	14.71	13.84
AVG	37.0287	35.7663	34.4408

Table 4.11: Percentage Profile loss for localized rough suction blade

Y/S	LOCALIZED ROUGH SUCTION SURFACE (300µm, 500µm, 750µm)			
	VEL=100 m/s	**VEL=250 m/s**	**VEL=300 m/s**	**VEL=350 m/s**
3.08	2.69	2.45	2.30	2.15
3.12	11.80	10.52	9.92	9.30
3.17	31.92	28.79	27.45	26.02
3.21	58.79	54.90	53.22	51.35
3.25	82.97	80.45	79.34	78.05
3.29	97.61	97.16	96.96	96.74
3.34	99.08	98.87	98.78	98.68
3.38	95.61	94.88	94.50	94.06
3.42	86.59	84.67	83.69	82.56
3.46	69.48	66.07	64.41	62.59
3.50	47.46	43.55	41.78	39.92
3.55	27.46	24.39	23.09	21.76
3.59	13.12	11.38	10.67	9.97
3.63	4.89	4.19	3.91	3.64
AVG	52.1133	50.1653	56.2897	48.3466

Table 4.12: Percentage Profile loss for localized rough pressure blade

Y/S	LOCALIZED ROUGH PRESSURE SURFACE			
	VEL= 100 m/s	**VEL=250 m/s**	**VEL=300 m/s**	**VEL=350 m/s**
3.08	2.52	2.52	1.95	2.22
3.12	11.45	10.33	9.37	9.20
3.17	31.27	28.04	26.86	25.67
3.21	58.22	53.56	52.95	50.44
3.25	82.63	78.97	79.28	76.68
3.29	97.53	96.52	96.81	95.81
3.34	99.20	98.77	99.05	98.70
3.38	96.09	95.56	95.15	94.96
3.42	87.51	86.13	84.69	84.09
3.46	70.78	68.09	65.66	64.39
3.50	48.72	45.25	42.90	41.26
3.55	28.48	25.58	23.94	22.61
3.59	13.75	12.05	11.17	10.44
3.63	5.17	4.50	4.09	3.83
AVG	52.3852	50.4242	49.5667	48.6000